



Efficient decentralized coordination of large-scale plug-in electric vehicle charging[☆]



Zhongjing Ma^a, Suli Zou^a, Long Ran^a, Xingyu Shi^a, Ian A. Hiskens^b

^a School of Automation, Beijing Institute of Technology (BIT), and the National Key Laboratory of Complex System Intelligent Control and Decision (BIT), Beijing 100081, China

^b Department of Electrical Engineering and Computer Science, University of Michigan, Ann Arbor, MI, USA

ARTICLE INFO

Article history:

Received 8 September 2013

Received in revised form

2 December 2015

Accepted 26 December 2015

Keywords:

Plug-in electric vehicles (PEVs)

Load control

Efficient power system operation

Decentralized optimization

Battery degradation

Distribution grid management

ABSTRACT

Minimizing the grid impacts of large-scale plug-in electric vehicle (PEV) charging tends to be associated with coordination strategies that seek to fill the overnight valley in electricity demand. However such strategies can result in high charging power, raising the possibility of local overloads within the distribution grid and of accelerated battery degradation. The paper establishes a framework for PEV charging coordination that facilitates the tradeoff between total generation cost and the local costs associated with overloading and battery degradation. A decentralized approach to solving the resulting large-scale optimization problem involves each PEV minimizing their charging cost with respect to a forecast price profile while taking into account local grid and battery effects. The charging strategies proposed by participating PEVs are used to update the price profile which is subsequently rebroadcast to the PEVs. The process then repeats. It is shown that under mild conditions this iterative process converges to the unique, efficient (socially optimal) coordination strategy.

© 2016 Elsevier Ltd. All rights reserved.

1. Introduction

As the population of plug-in electric vehicles (PEVs) grows, the electrical power drawn by chargers will begin to impact the grid. Numerous studies have explored the potential consequences of a high penetration of PEVs on the power grid (Denholm & Short, 2006; Hadley & Tsvetkova, 2008; Koyanagi & Uriu, 1997; Rahman & Shrestha, 1993; Yu, 2008). At the system-wide level, control strategies tend to focus on filling the overnight valley in background demand. A wider range of control objectives have been considered at the distribution level where uncoordinated charging may induce localized overloading, excessive losses and voltage

problems (Clement-Nyns, Haesen, & Driesen, 2010; Fernández, Román, Cossent, Domingo, & Frías, 2011; Galus & Andersson, 2008; Hermans, Almassalkhi, & Hiskens, 2012; Kelly, Rowe, & Wild, 2009). It is quite uncommon, however, to find studies that also take into account the effects of charging control on the health of the PEV batteries. This paper addresses the need for a charging coordination scheme which considers the tradeoffs between system-wide economic efficiency, distribution-level limitations and battery degradation concerns.

Charging behavior affects key battery characteristics, including the state of health, the resistance impedance growth and the cycle life, which are all strongly related to the energy capacity of a battery (Bashash, Moura, Forman, & Fathy, 2011; Wang et al., 2011). Intermittent charging may also shorten the battery lifespan (Gan, Topcu, & Low, 2012). Optimal charging strategies that take into account both the total energy cost and the battery state of health have been studied for single PEVs (Bashash et al., 2011; Cheng, Divakar, Wu, Ding, & Ho, 2011). These ideas form the basis for the extension, undertaken in this paper, to large-scale coordination.

Many studies have employed centralized methods for scheduling the charging power of PEVs, see Clement-Nyns et al. (2010), Galus and Andersson (2008) and Sundstrom and Binding (2010) and references therein. However individual PEVs are likely to desire autonomy, and optimizing over a large population of PEVs

[☆] This work was supported by the National Natural Science Foundation (NNSF) of China under Grant 61174091. The work was also supported by the International S&T Cooperation Program of China (ISTCP) through Grant 2015DFA61520, the US National Science Foundation through grant CNS-1238962 and the Department of Energy through award DE-PI0000012. The material in this paper was partially presented at the 54th IEEE Conference on Decision and Control, December 15–18, 2015, Osaka, Japan. This paper was recommended for publication in revised form by Editor Berç Rüstem.

E-mail addresses: mazhongjing@bit.edu.cn (Z. Ma), 20070192zsl@bit.edu.cn (S. Zou), 110992@bit.edu.cn (L. Ran), sxywd0602@aliyun.com (X. Shi), hiskens@umich.edu (I.A. Hiskens).

Table 1
List of key symbols.

\mathcal{T}	Charging horizon
\mathbf{u}_n	$(u_{nt}; t \in \mathcal{T})$, charging strategy of the n th PEV over the horizon \mathcal{T}
$\ \mathbf{u}_n\ _1$	$\sum_{t \in \mathcal{T}} u_{nt}$, total energy delivered to the n th PEV over the horizon \mathcal{T}
\mathbf{u}_n^{**}	Efficient charging strategy for PEV n
\mathbf{p}^{**}	Generation marginal cost with respect to \mathbf{u}^{**}
$\mathbf{u}_n^*(\mathbf{p})$	Optimal charging strategy of the n th PEV with respect to price profile \mathbf{p}

will have high computational complexity. Therefore centralized scheduling may be impractical. As an alternative, decentralized methods preserve individual authority and distribute the computational burden (Gan, Topcu, & Low, 2013; Ma, Callaway, & Hiskens, 2013).

Time-based strategies for scheduling PEV charging have difficulty effectively filling the night-time demand valley (Callaway & Hiskens, 2011). Likewise, strategies that rely on a fixed price schedule tend to result in suboptimal demand patterns. In contrast, this paper is motivated by a real-time price model which has been widely applied for demand response management (Mohsenian-Rad & Leon-Garcia, 2010; Samadi, Mohsenian-Rad, Schober, Wong, & Jatskevich, 2010) and electric vehicle charging/discharging coordination (Fan, 2012; Gan, Chen, Wierman, Topcu, & Low, 2013; Waraich et al., 2009; Wu, Mohsenian-Rad, & Huang, 2012). In this formulation, the electricity price is given by the generation marginal cost as a function of the total demand.

In the decentralized approach to charging coordination proposed in this paper, participating PEVs simultaneously determine their optimal charging strategy with respect to an energy price forecast. These proposed charging strategies are used to estimate the total demand over the charging horizon. An updated price forecast is obtained as a weighted average of the previous price forecast and the generation marginal cost evaluated at this latest demand forecast. The revised price is (re)broadcast to the PEVs, and the process repeats. This scheme is formalized in Section 4 where it is shown that convergence is guaranteed under mild conditions. Upon convergence, the price profile is coincident with the generation marginal cost over the charging horizon. As a consequence, the resulting collection of PEV charging strategies is efficient (socially optimal). Moreover, convergence is obtained without the need for artificial deviation costs to damp oscillations, as in Ma et al. (2013) and Gan et al. (2013). Cost terms introduced to mitigate the effects of local demand peaks and battery degradation play the same role as congestion pricing used for traffic control in communication networks (Kelly, Maulloo, & Tan, 1998), which has been adopted in Fan (2012) to schedule PEV charging.

The paper is organized as follows. Section 2 formalizes the concept of charging strategies, and motivates the costs associated with peak demand reduction and battery degradation. Centralized (socially optimal) coordination of PEV charging is considered in Section 3. A novel decentralized charging coordination algorithm is presented in Section 4 and convergence is analyzed. Simulations in Section 5 illustrate various characteristics of the algorithm. Section 6 concludes the paper and discusses ongoing research. A summary of the key notation used throughout the paper is provided in Table 1.

2. Formulation of PEV charging coordination

2.1. Admissible charging strategies

Consider the charging control of a large population of PEVs, $\mathcal{N} \equiv \{1, \dots, N\}$, over the horizon $\mathcal{T} \equiv \{0, \dots, T - 1\}$. For each PEV, $n \in \mathcal{N}$, the charging power over the time period $t \in \mathcal{T}$

is denoted by u_{nt} (with units of kW).¹ A charging strategy $\mathbf{u}_n \equiv (u_{nt}; t \in \mathcal{T})$ is *admissible* if,

$$u_{nt} \begin{cases} \geq 0, & t \in \mathcal{T}_n \\ = 0, & t \in \mathcal{T} \setminus \mathcal{T}_n, \end{cases} \quad (1a)$$

and

$$\|\mathbf{u}_n\|_1 \equiv \sum_{t \in \mathcal{T}} u_{nt} \leq \Gamma_n, \quad (1b)$$

where $\mathcal{T}_n \subset \mathcal{T}$ is the charging horizon and Γ_n is the energy capacity of the n th PEV. The parameters \mathcal{T}_n and Γ_n are determined by external factors such as driving style and vehicle type (Lee, Bareket, & Gordon, 2012). The set of admissible charging controls for the n th PEV is denoted by \mathcal{U}_n .

Coordination of PEV charging across a large population has generally sought to minimize total generation cost over the charging horizon, see for example Denholm and Short (2006), Gan et al. (2013) and Ma et al. (2013). In contrast, the coordination strategies developed in this paper seek to manage the tradeoff between total generation cost and local costs arising from high distribution-level demand and PEV battery degradation. These latter costs will now be discussed.

2.2. Demand charge

Distribution-level impacts of PEV charging include line and transformer overloading, low voltages and increased losses. All these effects are a consequence of coincident high charger power demand u_{nt} . Therefore undesirable distribution-grid effects can be minimized by encouraging PEVs to charge at lower power levels. This can be achieved by introducing a demand charge,

$$\text{Cost}_{demand,nt} = g_{demand,nt}(u_{nt}) \quad (2)$$

whereby PEVs incur a higher cost as their charging power increases, i.e. $g_{demand,nt}(\cdot)$ is a strictly increasing function. This charge is in addition to the cost of the energy delivered to the battery, and is consistent with existing tariff structures for larger consumers (Deliso, 2013).

2.3. Battery degradation cost

The LiFePO₄ lithium-ion battery has been widely used in a variety of electrical vehicles. A degradation cost model for LiFePO₄ battery cells is formulated in Forman, Stein, and Fathy (2013), based on the evolution of battery cell characteristics developed in Forman, Moura, Stein, and Fathy (2012) and Moura, Forman, Bashash, Stein, and Fathy (2011). This degradation model expresses the energy capacity loss per second (in Amp \times Hour \times Sec⁻¹) of a cell with respect to the charging current I and voltage V :

$$\partial_{cell}(I, V) = \beta_1 + \beta_2 I + \beta_3 V + \beta_4 I^2 + \beta_5 V^2 + \beta_6 IV + \beta_7 V^3, \quad (3)$$

with the parameters β_i , $i = 1, \dots, 7$, specified in Forman et al. (2013, Table I). The degradation cost for a battery cell charging at constant I and V for a period ΔT Sec is therefore,

$$g_{cell}(I, V) = P_{cell} \Delta T V_{cell} \partial_{cell}(I, V) \quad (4)$$

where P_{cell} is the price (\$/Wh) of battery cell capacity.

The cell voltage V_{cell} of a lithium-ion battery changes with its state of charge (SoC) (Kim, Seo, Chun, Cho, & Lee, 2012; Proisini, 2005). More specifically, as the SoC of a cell varies from zero to a very low value $soC_\ell > 0$, V_{cell} rises rapidly from zero to its nominal

¹ If the t th time period has length ΔT , then the energy delivered over that period is $u_{nt} \Delta T$.

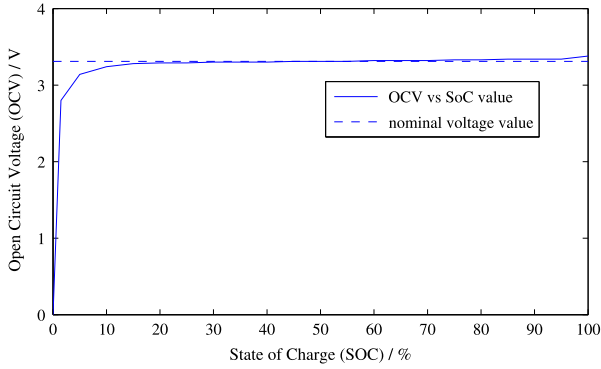


Fig. 1. Variation of the open circuit voltage of a LiFePO₄-type battery cell with respect to the SoC.

value V_{nom} , and remains near that value until the cell SoC reaches a high value soC_h (Cheng et al., 2011; Lu, Han, Li, Hua, & Ouyang, 2013; Singh, Izadian, & Anwar, 2013). Fig. 1 provides an illustration. Over the usable SoC range $soC_\ell \leq soC \leq soC_n$, the cell voltage remains almost constant, $V_{cell} \approx V_{nom}$.²

Assume that the battery pack of the n th PEV is composed of M_n identical cells, with all cells having the same SoC and charging power. At time t , each cell will have a charging current of $I = 10^3 u_{nt} / (M_n V_{nom})$, with u_{nt} in kW. The battery degradation cost of the n th PEV at time t can then be expressed as,

$$\begin{aligned} Cost_{degrad,nt} &= g_{cell,n}(u_{nt}) = M_n g_{cell} \left(\frac{10^3 u_{nt}}{M_n V_{nom}}, V_{nom} \right) \\ &= a_n u_{nt}^2 + b_n u_{nt} + c_n \end{aligned} \quad (5)$$

with

$$a_n = 10^6 P_{cell} \Delta T \beta_4 / (M_n V_{nom})$$

$$b_n = 10^3 P_{cell} \Delta T (\beta_2 + \beta_6 V_{nom})$$

$$c_n = M_n P_{cell} \Delta T V_{nom} (\beta_1 + \beta_3 V_{nom} + \beta_5 V_{nom}^2 + \beta_7 V_{nom}^3).$$

This gives the monetary loss incurred by charging at a rate of u_{nt} for the period ΔT .

3. Centralized PEV charging coordination

3.1. Formulation

The coordination problem of interest considers the tradeoff between the total cost of supplying energy to the PEV population and the benefit derived from doing so. The total cost is composed of the generation cost, the demand charge discussed in Section 2.2, and the PEV battery degradation cost formulated in Section 2.3. Coordination must ensure that all charging controls are admissible, $\mathbf{u}_n \in \mathcal{U}_n$ for all $n \in \mathcal{N}$.

Given a collection of admissible charging strategies $\mathbf{u} \in \mathcal{U}$, the system cost function can be expressed as,

$$\begin{aligned} J(\mathbf{u}) &\triangleq \sum_{t \in \mathcal{T}} \left\{ c \left(d_t + \sum_{n \in \mathcal{N}} u_{nt} \right) + \sum_{n \in \mathcal{N}} g_{nt}(u_{nt}) \right\} \\ &\quad - \sum_{n \in \mathcal{N}} \left\{ h_n(\|\mathbf{u}_n\|_1) \right\}, \end{aligned} \quad (6)$$

where:

- $c(\cdot)$ gives the generation cost with respect to the total demand $d_t + \sum_{n \in \mathcal{N}} u_{nt}$, and d_t denotes the aggregate inelastic base demand at time t ;

- $g_{nt}(u_{nt}) = g_{demand,nt}(u_{nt}) + g_{cell,n}(u_{nt})$ captures the demand charge (2) and battery degradation cost (5) of the n th PEV; and,
- $h_n(\|\mathbf{u}_n\|_1)$ denotes the benefit function of the n th PEV with respect to the total energy delivered over the charging horizon. In Han, Han, and Sezaki (2010), this function has the quadratic form,

$$h_n(\|\mathbf{u}_n\|_1) = -\delta_n (\|\mathbf{u}_n\|_1 - \Gamma_n)^2, \quad (7)$$

with the factor δ_n reflecting the relative importance of delivering the full charge to the PEV over the charging horizon.

The utility function of the n th PEV, for a charging strategy $\mathbf{u}_n \in \mathcal{U}_n$, can be written,

$$v_n(\mathbf{u}_n) \triangleq h_n(\|\mathbf{u}_n\|_1) - \sum_{t \in \mathcal{T}} g_{nt}(u_{nt}). \quad (8)$$

The system cost $J(\mathbf{u})$ given by (6) can then be rewritten:

$$J(\mathbf{u}) = \sum_{t \in \mathcal{T}} c \left(d_t + \sum_{n \in \mathcal{N}} u_{nt} \right) - \sum_{n \in \mathcal{N}} v_n(\mathbf{u}_n). \quad (9)$$

The individual utility function (8) is similar to that specified in Fan (2012), where a distributed PEV charging algorithm was developed based on congestion pricing concepts from internet traffic control (Kelly et al., 1998).

It is commonly assumed, see Bompard, Ma, Napoli, and Abrate (2007), Gountis and Bakirtzis (2004) and Wen and David (2001) and references therein, that the electricity generation cost can be approximated by the quadratic form,

$$c(y_t) = \frac{1}{2} a y_t^2 + b y_t + c, \quad (10)$$

with parameters a , b and c which reflect system conditions. The marginal generation cost, which is the derivative of generation cost, therefore varies linearly with the total demand, $p(y_t) \triangleq c'(y_t) = a y_t + b$.

Centralized PEV charging coordination can be formulated as the optimization problem:

Optimization Problem 1.

$$\min_{\mathbf{u} \in \mathcal{U}} J(\mathbf{u}). \quad (11)$$

The objective is to implement a socially optimal collection of charging strategies for all PEVs, denoted by \mathbf{u}^{**} , that minimizes the system cost (6) or its equivalent form (9). ■

The following assumptions will apply throughout the paper:

- (A1) $c(\cdot)$ is monotonically increasing, strictly convex and differentiable.
- (A2) $g_{nt}(\cdot)$, for all $n \in \mathcal{N}$, $t \in \mathcal{T}$, is monotonically increasing, strictly convex and differentiable. ■

When the benefit function takes the form (7), the solution obtained by minimizing $J(\mathbf{u})$ subject only to (1a) always satisfies (1b), and hence is also the solution for Optimization Problem 1. To see this, define the set of charging strategies that satisfy (1a) for the n th PEV,

$$\mathcal{S}_n \triangleq \{ \mathbf{u}_n \equiv (u_{nt}; t \in \mathcal{T}) ; \text{ s.t. constraint (1a)} \},$$

and let \mathcal{S} denote the collection of such sets for all $n \in \mathcal{N}$. Consider the optimization problem $\min_{\mathbf{u} \in \mathcal{S}} J(\mathbf{u})$ rather than (11).

Based on Assumptions (A1, A2), the efficient (socially optimal) charging behavior is unique and can be characterized by its associated KKT conditions (Boyd & Vandenberghe, 2004). The optimal solution \mathbf{u}^{**} is therefore given by:

$$\frac{\partial}{\partial u_{nt}} J(\mathbf{u}) \geq 0, \quad u_{nt} \geq 0, \quad \frac{\partial}{\partial u_{nt}} J(\mathbf{u}) u_{nt} = 0, \quad (12)$$

² Accordingly, it is difficult to accurately estimate the SoC of LiFePO₄ batteries from observations of their open circuit voltage.

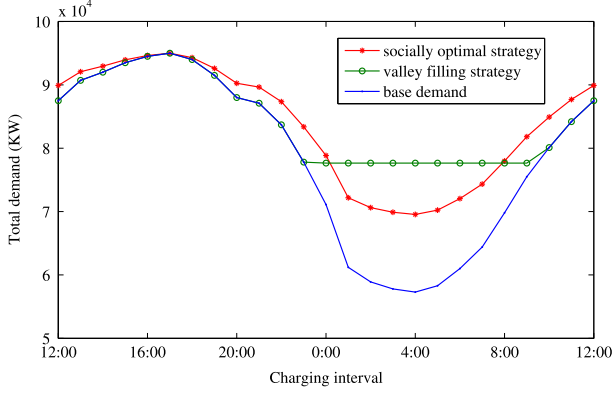


Fig. 2. Aggregate demand due to the efficient charging strategies.

for all $n \in \mathcal{N}$ and $t \in \mathcal{T}_n$, where:

$$\frac{\partial}{\partial u_{nt}} J(\mathbf{u}) = c'(d_t + \sum_{n \in \mathcal{N}} u_{nt}) - \frac{\partial}{\partial u_{nt}} v_n(\mathbf{u}_n).$$

It follows from (12) that the efficient charging behavior \mathbf{u}^{**} is uniquely specified by:

$$p_t^{**} \begin{cases} = \frac{\partial}{\partial u_{nt}} v_n(\mathbf{u}_n^{**}), & \text{when } u_{nt}^{**} > 0, \\ \geq \frac{\partial}{\partial u_{nt}} v_n(\mathbf{u}_n^{**}), & \text{when } u_{nt}^{**} = 0, \end{cases} \quad (13)$$

where $p_t^{**} = c'(d_t + \sum_{n \in \mathcal{N}} u_{nt}^{**})$ is the generation marginal cost over the charging horizon with respect to the efficient allocation \mathbf{u}^{**} .

Notice that if $\|\mathbf{u}_n^{**}\|_1 \geq \Gamma_n$ then (7) together with Assumption (A2) ensure that $\frac{\partial}{\partial u_{nt}} v_n(\mathbf{u}_n^{**}) < 0$. But $p_t^{**} > 0$ according to Assumption (A1), so (13) implies that $\mathbf{u}_n^{**} = \mathbf{0}$. Hence a contradiction. Accordingly, $\|\mathbf{u}_n^{**}\|_1 < \Gamma_n$ and (1b) is always satisfied.

3.2. Numerical example

This example considers coordinated charging of a population of 5000 PEVs over a common charging interval from noon on one day to noon on the next. In accordance with (10), the generation cost function has the quadratic form,

$$c(y_t) = 2.9 \times 10^{-7} y_t^2 + 0.06 y_t, \quad (14)$$

where $y_t = d_t + \sum_{n \in \mathcal{N}} u_{nt}$. The base demand \mathbf{d} , which is shown in Fig. 2, is representative of a typical hot summer day.

The battery pack of each PEV is composed of LiFePO₄ lithium-ion cells which have a nominal voltage of 3.3 V and energy capacity of 2.5 A h (Amp × Hour). These are typical values for batteries that are used in PEVs. Assume the price of battery cell capacity is \$10/Wh. Furthermore, let all PEVs have battery capacity of 40 kWh. Then the battery degradation cost (5) for each PEV is given (approximately) by,

$$g_{cell,n}(u_{nt}) = 0.0012u_{nt}^2 + 0.11u_{nt} - 0.02.$$

Each PEV is subject to a quadratic demand charge $g_{demand,nt}(u_{nt}) = 0.0018u_{nt}^2$. Thus, the local costs incurred by each PEV at time t amount to,

$$g_{nt}(u_{nt}) = 0.003u_{nt}^2 + 0.11u_{nt} - 0.02. \quad (15)$$

Initially all PEVs use the same weighting factor $\delta_n = 0.03$ in their utility function $v_n(\mathbf{u}_n)$ given by (7) and (8). This will be relaxed in later investigations.

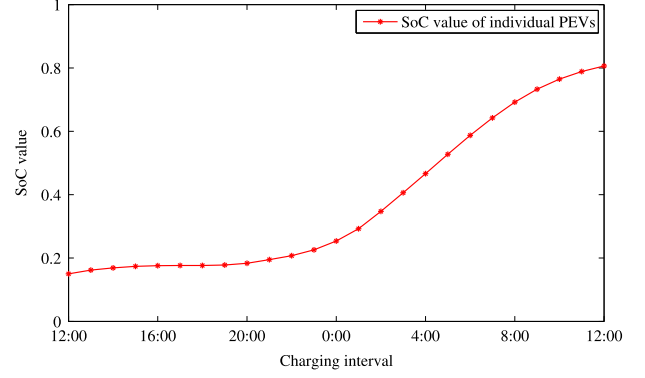


Fig. 3. Evolution of the SoC of an individual PEV.

For simplicity, assume all PEVs have identical minimum and maximum SoC, with $soC_\ell = 15\%$ and $soC_h = 90\%$. The upper limit (1b) on the energy that can be delivered to each PEV is given by,

$$\Gamma_n = 40(soC_h - soC_{n0}),$$

which equals 30 kWh if $soC_{n0} = soC_\ell = 15\%$ for all n .

The efficient (socially optimal) charging strategies given by (11), \mathbf{u}_n^{**} for $n \in \mathcal{N}$, result in the aggregate demand shown in Fig. 2. The evolution of the SoC of one of the PEVs is shown in Fig. 3. As a comparison, the aggregate demand of the valley-filling strategy \mathbf{u}^{vf} given by Ma et al. (2013) is also shown in Fig. 2. Note that the algorithm developed in Ma et al. (2013) enforces an equality constraint on the energy delivered, $\|\mathbf{u}_n^{vf}\|_1 = \Gamma_n^{vf}$, rather than incorporating a benefit function of the form (7). Therefore, to ensure a meaningful comparison, the total charge requirement in the valley-filling case was set equal to the energy delivered in the socially optimal solution, $\Gamma_n^{vf} = \|\mathbf{u}_n^{**}\|_1$.

The socially optimal charging strategy given by (11) establishes a tradeoff between the total generation cost of the system and the local costs (demand charge and battery degradation cost) of the PEV population. As illustrated in Fig. 2, this results in an outcome that differs quite considerably from the valley-filling strategy which is solely concerned with minimizing total generation cost. This distortion away from valley-filling increases as higher weighting is given to the local costs of the PEV population.

This difference between the socially optimal and valley-filling strategies can be quantified by considering,

$$\begin{aligned} \sum_{t \in \mathcal{T}} c(d_t + \sum_{n \in \mathcal{N}} u_{nt}^{**}) - \sum_{t \in \mathcal{T}} c(d_t + \sum_{n \in \mathcal{N}} u_{nt}^{vf}) &= 211.7 \\ \sum_{n \in \mathcal{N}} \sum_{t \in \mathcal{T}} g_{nt}(u_{nt}^{**}) - \sum_{n \in \mathcal{N}} \sum_{t \in \mathcal{T}} g_{nt}(u_{nt}^{vf}) &= -671.3 \end{aligned}$$

where the constraint $\Gamma_n^{vf} = \|\mathbf{u}_n^{**}\|_1$ has been taken into account. It can be seen that incorporating the local costs resulted in an increase in generation cost of \$211.7/day. However this was more than offset by a reduction in the local costs of \$671.3/day, resulting in an overall saving of \$459.6/day. As a further comparison, if $\Gamma_n^{vf} = \Gamma_n$, i.e. PEVs must fully charge rather than settle for the reduced energy delivery of $\|\mathbf{u}_n^{**}\|_1$, then adopting \mathbf{u}^{**} instead of \mathbf{u}^{vf} would result in a cost saving of \$1640.2/day.

The following investigations consider the effects of variations in the battery degradation cost $g_{cell,n}$ and the benefit function h_n on the optimal charging strategies of a population of PEVs.

Fig. 4 shows the evolution of the (efficient) aggregate demand as the battery price P_{cell} is varied. For this study, the demand charge (2) was set to zero and $\delta_n = 0.03$ in all cases. It can be seen that the efficient aggregate demand approaches valley-filling as P_{cell} decreases, and becomes exactly valley-filling when $P_{cell} = 0$.

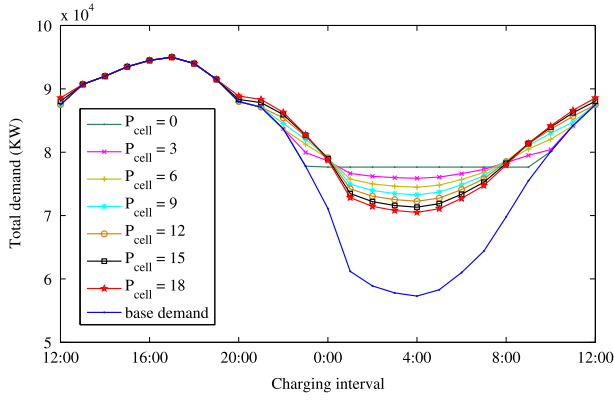


Fig. 4. Aggregate demand for efficient charging strategies as battery price P_{cell} varies.

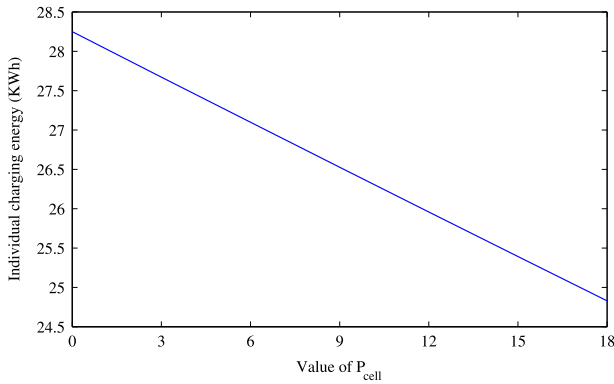


Fig. 5. Total delivered energy $\|\mathbf{u}_n\|_1$ for an individual PEV as battery price P_{cell} varies.

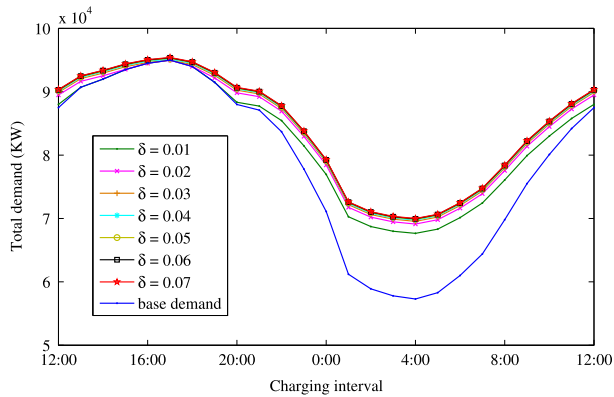


Fig. 6. Aggregate demand for efficient charging strategies as the benefit function parameter δ_n varies.

Fig. 5 shows that the total delivered energy $\|\mathbf{u}_n\|_1$ decreases as P_{cell} increases.

Fig. 6 shows the variation in the efficient aggregate demand as the benefit function parameter δ_n is varied. The general shape of the aggregate demand remains largely unchanged. It is shown in Fig. 7 that the total delivered energy $\|\mathbf{u}_n\|_1$ increases with δ_n , approaching the energy capacity limit T_n .

4. Decentralized charging coordination method for PEV populations

Centralized coordination is only possible when the system operator has complete information, including the characteristics of PEV batteries and the valuation functions of individual PEVs.

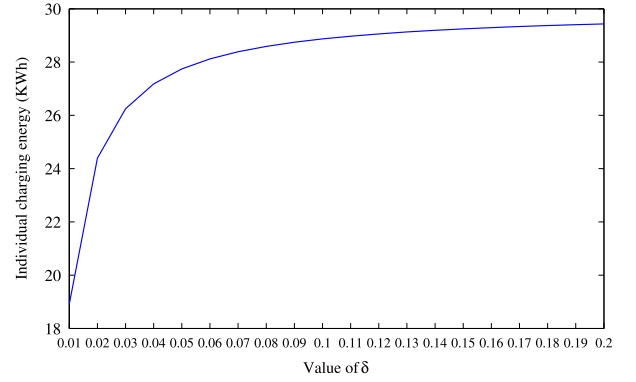


Fig. 7. Total delivered energy $\|\mathbf{u}_n\|_1$ for an individual PEV as the benefit function parameter δ_n varies.

It is unlikely, however, that individuals would be willing to share such private information. Also, for a large population, centralized control may be computationally infeasible. Thus, the remainder of the paper is devoted to the development of a decentralized coordination process where each PEV updates its charging strategy with respect to a common electricity price profile, and then the price profile is updated based on the latest charging strategies for the population.

Decentralized coordination of PEV charging can be achieved using an algorithm of the form:

- (S1) Each PEV autonomously determines its optimal charging strategy with respect to a given electricity price profile $\mathbf{p} \equiv (p_t, t \in \mathcal{T})$. This optimal strategy takes into account the tradeoff between the electricity cost and local (demand and battery degradation) costs over the entire charging horizon.
- (S2) The electricity price profile \mathbf{p} is updated to reflect the latest charging strategies determined by the PEV population in (S1).
- (S3) Steps (S1) and (S2) are repeated until the change in the price profile at (S2) is negligible.

Section 4.1 establishes the optimal charging strategy $\mathbf{u}_n^*(\mathbf{p})$ of each PEV, $n \in \mathcal{N}$, with respect to a given price profile \mathbf{p} . A mechanism for updating the electricity price profile is designed in Section 4.2. Section 4.3 then formalizes the algorithm (S1)–(S3), establishes convergence properties, and shows that decentralized coordination gives the socially optimal (economically efficient) charging strategy.

4.1. Optimal response of each PEV with respect to a fixed price profile

The individual cost function of the n th PEV, under charging strategy $\mathbf{u}_n \in \mathcal{U}_n$ and with respect to the price profile \mathbf{p} , can be written:

$$J_n(\mathbf{u}_n; \mathbf{p}) \triangleq \sum_{t \in \mathcal{T}} p_t u_{nt} - v_n(\mathbf{u}_n). \quad (16)$$

Alternatively, using (8), this cost function can be expressed in the form:

$$J_n(\mathbf{u}_n; \mathbf{p}) = \sum_{t \in \mathcal{T}} \{p_t u_{nt} + g_{nt}(u_{nt})\} - h_n \left(\sum_{t \in \mathcal{T}} u_{nt} \right),$$

where it becomes clear that the cost is composed of the total electricity cost $\sum_{t \in \mathcal{T}} p_t u_{nt}$, the total local cost $\sum_{t \in \mathcal{T}} g_{nt}(u_{nt})$, and the benefit derived from the total energy delivered over the charging horizon $h_n \left(\sum_{t \in \mathcal{T}} u_{nt} \right)$.

The optimal charging strategy of the n th PEV, with respect to \mathbf{p} , is obtained by minimizing the cost function (16),

$$\mathbf{u}_n^*(\mathbf{p}) = \underset{\mathbf{u}_n \in \mathcal{U}_n}{\operatorname{argmin}} J_n(\mathbf{u}_n; \mathbf{p}). \quad (17)$$

It will be shown in [Theorem 4.1](#) that the optimal response of the n th PEV has the form:

$$u_{nt}(\mathbf{p}, A_n) = \begin{cases} \max\{0, [g'_{nt}]^{-1}(A_n - p_t)\}, & t \in \mathcal{T}_n \\ 0, & t \in \mathcal{T} \setminus \mathcal{T}_n \end{cases} \quad (18)$$

for some A_n , where g'_{nt} is the derivative of g_{nt} , and $[g'_{nt}]^{-1}$ is the corresponding inverse function. Since the total charging energy is elastic, the value of A_n is dependent upon the PEV specifications and the price \mathbf{p} , with this dependence established in [Theorem 4.1](#).

Determining the optimal charging strategy (17) proceeds as follows. [Lemma 4.1](#) addresses the restricted problem of finding the optimal charging strategy when the total delivered energy takes a specified value, $\|\mathbf{u}_n\|_1 = \omega$, where $0 \leq \omega \leq \Gamma_n$. [Lemma 4.2](#) considers the charging strategy in the form (18) and establishes the relationship between the value of A_n and the total energy delivered $\|\mathbf{u}_n(\mathbf{p}, A_n)\|_1$. [Lemma 4.3](#) shows that the sensitivity of charging cost to changes in ω is given by A_n . Finally, [Theorem 4.1](#) brings all the results together and determines the unique value of A_n that ensures (18) is optimal in the sense of (17).

To begin with, consider the cost for the n th PEV, but excluding h_n . This can be written,

$$F_n(\mathbf{u}_n; \mathbf{p}) \triangleq \sum_{t \in \mathcal{T}} \{p_t u_{nt} + g_{nt}(u_{nt})\}. \quad (19)$$

This function will be used to examine scenarios where the total charging is constant, $\|\mathbf{u}_n\|_1 = \omega$. In such cases, the cost $h_n(\|\mathbf{u}_n\|_1)$ can be neglected since it is equal across all such scenarios. Accordingly, define the set of charging strategies where total energy ω is delivered to the n th PEV as,

$$\mathcal{U}_n(\omega) \triangleq \{\mathbf{u}_n \in \mathcal{U}_n; \text{ s.t. } \|\mathbf{u}_n\|_1 = \omega\}. \quad (20)$$

Lemma 4.1. Consider a fixed ω , with $0 \leq \omega \leq \Gamma_n$, and a fixed \mathbf{p} . Then $\mathbf{u}_n(\mathbf{p}, A_n)$, defined in (18), is the unique charging strategy minimizing the cost function (19) subject to the set of admissible charging strategies $\mathcal{U}_n(\omega)$.

Proof. Define the Lagrangian function,

$$L_n(\mathbf{u}_n, A_n; \mathbf{p}) \triangleq F_n(\mathbf{u}_n; \mathbf{p}) + A_n(\omega - \|\mathbf{u}_n\|_1), \quad (21)$$

with $u_{nt} \geq 0$ for $t \in \mathcal{T}$, and A_n the Lagrangian multiplier associated with the constraint on total delivered energy (20). The desired optimal strategy must satisfy the KKT conditions ([Boyd & Vandenberghe, 2004](#)):

- (i) $\frac{\partial L_n}{\partial A_n} = 0$.
- (ii) $\frac{\partial L_n}{\partial u_{nt}} \geq 0$, $u_{nt} \geq 0$, with complementary slackness.

The equality (i) recovers the constraint on total energy $\|\mathbf{u}_n\|_1 = \omega$, while the inequalities given in (ii) can be expressed in the form,

$$p_t + g'_{nt}(u_{nt}) - A_n \begin{cases} = 0, & \text{when } u_{nt} > 0 \\ \geq 0, & \text{otherwise,} \end{cases} \quad (22)$$

which is equivalent to (18). Moreover, since $F_n(\mathbf{u}_n; \mathbf{p})$ is convex with respect to \mathbf{u}_n , the optimal charging strategy defined by (18) must be unique for a given $\mathcal{U}_n(\omega)$. ■

This lemma establishes the minimum (17) when \mathbf{u}_n is restricted to $\mathcal{U}_n(\omega)$, for a specified value of ω . Relaxing that restriction, by allowing $\mathbf{u}_n \in \mathcal{U}_n$, is achieved in [Theorem 4.1](#). Before reaching that point, it is necessary to establish some notation and intermediate results.

For any PEV, $n \in \mathcal{N}$, the pair of values $A_n^-(\mathbf{p})$ and $A_n^+(\mathbf{p})$ are defined as:

$$A_n^-(\mathbf{p}) = \max\{A, \text{ such that } \|\mathbf{u}_n(\mathbf{p}, A)\|_1 = 0\} \quad (23)$$

$$A_n^+(\mathbf{p}) = A, \quad \text{such that } \|\mathbf{u}_n(\mathbf{p}, A)\|_1 = \Gamma_n. \quad (24)$$

Note that the subscript n is included on A_n^- for consistency, though it is independent of n .

The following lemma establishes a few basic relationships between the Lagrangian multiplier A_n and the minimizing control strategy.

Lemma 4.2. Consider a fixed price profile \mathbf{p} . Then:

- (i) Every $u_{nt}(\mathbf{p}, A_n)$, $t \in \mathcal{T}$, is non-decreasing with $A_n \in \mathbb{R}$, and hence $\|\mathbf{u}_n(\mathbf{p}, A_n)\|_1$ is non-decreasing with A_n . Furthermore, $\|\mathbf{u}_n(\mathbf{p}, A_n)\|_1$ is strictly increasing for $A_n \geq A_n^-(\mathbf{p})$.
- (ii) $\mathbf{u}_n(\mathbf{p}, A_n)$ is admissible for $A_n^-(\mathbf{p}) \leq A_n \leq A_n^+(\mathbf{p})$, but not admissible for any $A_n > A_n^+(\mathbf{p})$.

Proof. Property (i) holds by the specification of $u_{nt}(\mathbf{p}, A_n)$ given in (18) and verified by [Lemma 4.1](#), keeping in mind Assumption (A2). From (23) and (24), $\|\mathbf{u}_n(\mathbf{p}, A_n^-(\mathbf{p}))\|_1 = 0$ and $\|\mathbf{u}_n(\mathbf{p}, A_n^+(\mathbf{p}))\|_1 = \Gamma_n$. Therefore, since $\|\mathbf{u}_n(\mathbf{p}, A_n)\|_1$ is strictly increasing for $A_n \geq A_n^-(\mathbf{p})$, it follows that:

- $u_{nt}(\mathbf{p}, A_n) \geq 0$ for all $t \in \mathcal{T}$, and $\|\mathbf{u}_n(\mathbf{p}, A_n)\|_1 \leq \Gamma_n$ for $A_n^-(\mathbf{p}) \leq A_n \leq A_n^+(\mathbf{p})$, so $\mathbf{u}_n(\mathbf{p}, A_n)$ is admissible.
- $\|\mathbf{u}_n(\mathbf{p}, A_n)\|_1 > \Gamma_n$ when $A_n > A_n^+(\mathbf{p})$, so $\mathbf{u}_n(\mathbf{p}, A_n)$ is not admissible.

This establishes property (ii). ■

[Lemma 4.2](#) guarantees that for a fixed \mathbf{p} , $\|\mathbf{u}_n(\mathbf{p}, A_n)\|_1$ strictly increases from 0 to Γ_n on the interval $A_n \in [A_n^-(\mathbf{p}), A_n^+(\mathbf{p})]$. This implies that $\|\mathbf{u}_n(\mathbf{p}, A)\|_1$ is invertible on $[A_n^-(\mathbf{p}), A_n^+(\mathbf{p})]$, with the inverse denoted:

$$\mathcal{A}_n(\mathbf{p}, \cdot) : [0, \Gamma_n] \rightarrow [A_n^-(\mathbf{p}), A_n^+(\mathbf{p})]. \quad (25)$$

It follows that $\mathcal{A}_n(\mathbf{p}, \omega)$ is strictly increasing with ω and,

$$\mathcal{A}_n(\mathbf{p}, \omega) = A_n \iff \|\mathbf{u}_n(\mathbf{p}, A_n)\|_1 = \omega. \quad (26)$$

The charging strategy that satisfies (18) and delivers total energy of ω will be denoted by $\mathbf{u}_n(\mathbf{p}, \mathcal{A}_n(\mathbf{p}, \omega))$, and therefore $\|\mathbf{u}_n(\mathbf{p}, \mathcal{A}_n(\mathbf{p}, \omega))\|_1 = \omega$.

Because of the non-negativity constraint on u_{nt} and the corresponding complementary slackness requirement from [Lemma 4.1](#), it is not straightforward to determine a closed form expression for the function $\mathcal{A}_n(\mathbf{p}, \omega)$. A valuable property of $\mathcal{A}_n(\mathbf{p}, \omega)$ is, however, established in the following lemma.

Lemma 4.3. For any fixed price profile \mathbf{p} ,

$$\frac{d}{d\omega} F_n^*(\mathbf{p}, \omega) = \mathcal{A}_n(\mathbf{p}, \omega), \quad \text{with } \omega \in [0, \Gamma_n], \quad (27)$$

where,

$$F_n^*(\mathbf{p}, \omega) \triangleq \min_{\mathbf{u}_n \in \mathcal{U}_n(\omega)} F_n(\mathbf{u}_n; \mathbf{p}). \quad (28)$$

Proof. From (21), A_n is the Lagrangian multiplier associated with the constraint $\|\mathbf{u}_n\|_1 = \omega$. Based on duality theory ([Boyd & Vandenberghe, 2004](#)), the sensitivity of the minimum value $F_n^*(\mathbf{p}, \omega)$ with respect to changes in ω is therefore given by A_n . The result follows from (26). ■

It is now possible to establish the optimal charging strategy for a given \mathbf{p} . This is achieved in the following theorem, which implicitly determines the optimal value for ω in the process.

Theorem 4.1. Assume $h_n(\omega)$ is continuously differentiable, increasing and concave on $0 \leq \omega \leq \Gamma_n$. Define,

$$f_n(\mathbf{p}, \omega) \triangleq \mathcal{A}_n(\mathbf{p}, \omega) - h'_n(\omega) \quad (29)$$

with $\mathcal{A}_n(\mathbf{p}, \cdot)$ given by (25), and

$$A_n^*(\mathbf{p}) = \begin{cases} \mathcal{A}_n(\mathbf{p}, \Gamma_n), & \text{if } f_n(\mathbf{p}, \Gamma_n) \leq 0 \\ \mathcal{A}_n(\mathbf{p}, 0), & \text{if } f_n(\mathbf{p}, 0) \geq 0 \\ \mathcal{A}_n(\mathbf{p}, \omega^*), & \text{if } f_n(\mathbf{p}, \omega^*) = 0 \end{cases} \quad (30)$$

where $0 < \omega^* < \Gamma_n$. Then the charging strategy $\mathbf{u}_n(\mathbf{p}, A_n^*(\mathbf{p}))$ defined in (18) uniquely minimizes the cost function (16) with respect to a given \mathbf{p} , i.e. $\mathbf{u}_n^*(\mathbf{p}) = \mathbf{u}_n(\mathbf{p}, A_n^*(\mathbf{p}))$.

Proof. Recall that

$$J_n(\mathbf{u}_n; \mathbf{p}) = F_n(\mathbf{u}_n; \mathbf{p}) - h_n(\omega),$$

for all $\mathbf{u}_n \in \mathcal{U}_n(\omega)$. Then,

$$\begin{aligned} \min_{\mathbf{u}_n \in \mathcal{U}_n} J_n(\mathbf{u}_n; \mathbf{p}) &= \min_{\mathbf{u}_n \in \mathcal{U}_n} \{F_n(\mathbf{u}_n; \mathbf{p}) - h_n(\|\mathbf{u}_n\|_1)\} \\ &= F_n^*(\mathbf{p}, \omega^*) - h_n(\omega^*), \end{aligned}$$

where ω^* is the total charging energy that minimizes the cost function $J_n(\cdot; \mathbf{p})$. Note that ω^* is constrained to $0 \leq \omega^* \leq \Gamma_n$. For $0 < \omega^* < \Gamma_n$, the optimal energy demand ω^* is implicitly defined by the stationarity condition,

$$\frac{d}{d\omega} (F_n^*(\mathbf{p}, \omega) - h_n(\omega)) \Big|_{\omega=\omega^*} = f_n(\mathbf{p}, \omega^*) = 0 \quad (31)$$

where Lemma 4.3 has been used to establish the first equality. Moreover, $h'_n(\omega)$ decreases on ω , since h_n is assumed to be concave, and $\mathcal{A}_n(\mathbf{p}, \omega)$ is strictly increasing with ω . Therefore, if a solution for (31) exists over $0 < \omega^* < \Gamma_n$, then it must be unique.

If (31) cannot be satisfied for $0 < \omega < \Gamma_n$ then no stationary point exists over that open interval. Consequently, the cost $F_n^*(\mathbf{p}, \omega) - h_n(\omega)$ must exhibit monotonic behavior over $0 < \omega < \Gamma_n$. If the cost strictly increases with ω , so $\mathcal{A}_n(\mathbf{p}, \omega) - h'_n(\omega) = f_n(\mathbf{p}, \omega) > 0$ for $0 < \omega < \Gamma_n$, then the minimum cost solution will occur at the lower end, $\omega^* = 0$. Similarly, if the cost is strictly decreasing with ω , so the derivative $f_n(\mathbf{p}, \omega) < 0$ over $0 < \omega < \Gamma_n$, then the minimum cost solution will occur at the upper end, $\omega^* = \Gamma_n$. ■

4.2. Price profile update mechanism

If the price profile \mathbf{p} was equal to the optimal (efficient) generation marginal cost \mathbf{p}^{**} given by (13), then the collection of PEV charging strategies $\mathbf{u}^*(\mathbf{p}) \equiv (\mathbf{u}_n(\mathbf{p}, A_n^*(\mathbf{p})), n \in \mathcal{N})$ given by (18) and (30) would be efficient. However, this optimal price \mathbf{p}^{**} cannot be determined *a priori*. Hence there is a need for an update mechanism that guarantees convergence of the price profile to the efficient marginal cost \mathbf{p}^{**} . Consider the scheme,

$$p_t^+(\mathbf{p}) = p_t + \eta \left(c' \left(d_t + \sum_{n \in \mathcal{N}} u_{nt}^*(\mathbf{p}) \right) - p_t \right), \quad t \in \mathcal{T} \quad (32)$$

where $\eta > 0$ is a fixed parameter, and $\mathbf{u}_n^*(\mathbf{p})$, defined in (17), is the optimal charging strategy for the n th PEV with respect to \mathbf{p} .

Given a system price profile \mathbf{p} over the charging horizon \mathcal{T} , if p_t is lower than the generation marginal cost $c' \left(d_t + \sum_{n \in \mathcal{N}} u_{nt}^*(\mathbf{p}) \right)$ at time t , the system will set a higher price p_t^+ to encourage PEVs to reduce their charging demand at that time. Likewise, if p_t is higher than the marginal cost c' , the system will set a lower system price p_t^+ to encourage PEVs to increase their charging demand at that time.

Notice that the price update mechanism (32) can be written in the form,

$$\mathbf{p}^+ = (1 - \eta)\mathbf{p} + \eta\mathcal{P}(\mathbf{p}),$$

where

$$\mathcal{P}_t(\mathbf{p}) = c' \left(d_t + \sum_{n \in \mathcal{N}} u_{nt}^*(\mathbf{p}) \right), \quad t \in \mathcal{T}.$$

This price update iteration takes the form of the Krasnosel'skij iteration (Berinde, 2007; Grammatico, Parise, Colombino, & Lygeros, 0000), and is therefore guaranteed to converge to a fixed point of $\mathcal{P}(\cdot)$ for any $\eta \in (0, 1)$ if $\mathcal{P}(\cdot)$ is non-expansive. Corollary 4.1 establishes a more general sufficient condition under which the system converges to the unique price profile \mathbf{p}^{**} which is the efficient marginal cost.

4.3. Decentralized coordination of PEV charging

It is now possible to formalize a decentralized coordination algorithm for determining the optimal charging strategy for a population of PEVs.

Algorithm 1 (Decentralized Coordination).

- Specify the aggregate base demand \mathbf{d} ;
- Define an $\varepsilon_{\text{stop}}$ to terminate iterations;
- Initialize $\varepsilon > \varepsilon_{\text{stop}}$ and an initial price profile $\mathbf{p}^{(0)}$;
- Set $k = 0$;
- While $\varepsilon > \varepsilon_{\text{stop}}$
 - Determine the optimal charging profile $\mathbf{u}_n^{(k+1)}$ w.r.t. $\mathbf{p}^{(k)}$ for all $n \in \mathcal{N}$ PEVs simultaneously by minimizing the individual cost function (16),

$$\mathbf{u}_n^{(k+1)}(\mathbf{p}^{(k)}) \triangleq \operatorname{argmin}_{\mathbf{u}_n \in \mathcal{U}_n} \left\{ \sum_{t \in \mathcal{T}} p_t^{(k)} u_{nt} - v_n(\mathbf{u}_n) \right\};$$
 - Determine $\mathbf{p}^{(k+1)}$ from $\mathbf{p}^{(k)}$ and $\mathbf{u}^{(k+1)}(\mathbf{p}^{(k)})$ using (32),

$$p_t^{(k+1)} = p_t^{(k)} + \eta \left(c' \left(d_t + \sum_{n \in \mathcal{N}} u_{nt}^{(k+1)} \right) - p_t^{(k)} \right),$$
 for all $t \in \mathcal{T}$;
 - Update $\varepsilon := \|\mathbf{p}^{(k+1)} - \mathbf{p}^{(k)}\|_1$;
 - Update $k := k + 1$. ■

If Algorithm 1 converges, this decentralized process will achieve the efficient solution. Iterations could, however, be oscillatory or even divergent. In order to establish convergence, it is useful to define v_{nt} as the Lipschitz constant for the function $[g'_{nt}]^{-1}(\cdot)$ over the interval $[g'_{nt}(0), g'_{nt}(\Gamma_n)]$, with

$$v = \max_{n \in \mathcal{N}, t \in \mathcal{T}} v_{nt}, \quad (33)$$

and to define κ as the Lipschitz constant for $c'(\cdot)$ over the typical range in the total demand. The following intermediate result is also required.

Lemma 4.4. Assume the terminal valuation function h_n is increasing and strictly concave. Then,

$$\|\mathbf{u}_n^*(\mathbf{p}) - \mathbf{u}_n^*(\mathbf{q})\|_1 \leq 2v\|\mathbf{p} - \mathbf{q}\|_1 \quad (34)$$

where $\|\cdot\|_1$ denotes the l_1 norm of the associated vector.

The proof of Lemma 4.4 is given in Appendix A. ■

It is now possible to establish the convergence properties of Algorithm 1, and hence of the decentralized coordination process.

Corollary 4.1 (Convergence of Algorithm 1). Suppose $\alpha \equiv |1 - \eta| + 2N\kappa v\eta < 1$ and consider any initial charging price $\mathbf{p}^{(0)}$. Then Algorithm 1 converges to the efficient solution \mathbf{u}^{**} which is specified in (13). Moreover, for any $\varepsilon > 0$, the system converges to a price profile \mathbf{p} , such that $\|\mathbf{p} - \mathbf{p}^{**}\|_1 \leq \varepsilon$, in $K(\varepsilon)$ iterations, with

$$K(\varepsilon) = \left\lceil \frac{1}{\ln(\alpha)} \left(\ln(\varepsilon) - \ln(T) - \ln(Q_{\max}) \right) \right\rceil, \quad (35)$$

where Q_{\max} denotes the maximum possible price, and $\lceil x \rceil$ represents the minimal integer value larger than or equal to x .

Remarks:

- (i) In practice, convergence to the desired tolerance ε requires many fewer iterations than the upper bound established in (35). Typical convergence behavior is illustrated in Section 5.
- (ii) The upper bound on the iteration count, $K(\varepsilon)$, is of order $O(\ln(\varepsilon))$, and is independent of the size of the PEV population. The choice of α is influenced by the PEV population size, with the condition $\alpha < 1$ requiring that $N < \frac{1}{2\kappa v}$. Notice from (10), though, that $\kappa(N) \in O(\frac{1}{N^2})$ because the generation cost $c(\cdot)$ must remain finite as the PEV population N grows. Therefore this necessary condition on N is not restrictive.

Proof of Corollary 4.1. Consider a pair of price profiles \mathbf{p} and \mathbf{q} , and the respective updated price profiles \mathbf{p}^+ and \mathbf{q}^+ given by (32). Then,

$$\begin{aligned} & \|\mathbf{p}^+ - \mathbf{q}^+\|_1 \\ &= \sum_{t \in \mathcal{T}} \left| \left\{ p_t + \eta \left(c' \left(d_t + \sum_{n \in \mathcal{N}} u_{nt}^*(\mathbf{p}) \right) - p_t \right) \right\} \right. \\ & \quad \left. - \left\{ q_t + \eta \left(c' \left(d_t + \sum_{n \in \mathcal{N}} u_{nt}^*(\mathbf{q}) \right) - q_t \right) \right\} \right| \\ &= \sum_{t \in \mathcal{T}} \left| \eta \left(c' \left(d_t + \sum_{n \in \mathcal{N}} u_{nt}^*(\mathbf{p}) \right) - c' \left(d_t + \sum_{n \in \mathcal{N}} u_{nt}^*(\mathbf{q}) \right) \right) \right. \\ & \quad \left. + (1 - \eta)(p_t - q_t) \right| \\ &\leq \eta \sum_{t \in \mathcal{T}} \left| c' \left(d_t + \sum_{n \in \mathcal{N}} u_{nt}^*(\mathbf{p}) \right) - c' \left(d_t + \sum_{n \in \mathcal{N}} u_{nt}^*(\mathbf{q}) \right) \right| \\ & \quad + |1 - \eta| \times \|\mathbf{p} - \mathbf{q}\|_1. \end{aligned} \quad (36)$$

Also, given the definition of κ , it follows that,

$$\begin{aligned} & \sum_{t \in \mathcal{T}} \left| c' \left(d_t + \sum_{n \in \mathcal{N}} u_{nt}^*(\mathbf{p}) \right) - c' \left(d_t + \sum_{n \in \mathcal{N}} u_{nt}^*(\mathbf{q}) \right) \right| \\ &\leq \kappa \sum_{t \in \mathcal{T}} \left| \sum_{n \in \mathcal{N}} u_{nt}^*(\mathbf{p}) - \sum_{n \in \mathcal{N}} u_{nt}^*(\mathbf{q}) \right| \\ &\leq \kappa \sum_{t \in \mathcal{T}} \sum_{n \in \mathcal{N}} |u_{nt}^*(\mathbf{p}) - u_{nt}^*(\mathbf{q})| \\ &= \kappa \sum_{n \in \mathcal{N}} \sum_{t \in \mathcal{T}} |u_{nt}^*(\mathbf{p}) - u_{nt}^*(\mathbf{q})| \\ &= \kappa \sum_{n \in \mathcal{N}} \|\mathbf{u}_n^*(\mathbf{p}) - \mathbf{u}_n^*(\mathbf{q})\|_1 \\ &\leq 2\kappa v \sum_{n \in \mathcal{N}} \|\mathbf{p} - \mathbf{q}\|_1 \\ &= 2N\kappa v \|\mathbf{p} - \mathbf{q}\|_1 \end{aligned} \quad (37)$$

$$= 2N\kappa v \|\mathbf{p} - \mathbf{q}\|_1 \quad (38)$$

where the inequality (37) invokes Lemma 4.4. Inequalities (36) and (38) together imply,

$$\|\mathbf{p}^+ - \mathbf{q}^+\|_1 \leq (|1 - \eta| + 2N\kappa v \eta) \|\mathbf{p} - \mathbf{q}\|_1. \quad (39)$$

If $|1 - \eta| + 2N\kappa v \eta < 1$, then,

$$\|\mathbf{p}^+ - \mathbf{q}^+\|_1 < \|\mathbf{p} - \mathbf{q}\|_1, \quad (40)$$

so the price update operator $\mathbf{p}^+(\mathbf{p})$ specified in (32) is a contraction map. Hence by the contraction mapping theorem (Smart, 1974), the system price $\mathbf{p}^{(k)}$ converges to a unique price profile \mathbf{p}^* from any initial price profile $\mathbf{p}^{(0)}$. At the converged price, $\mathbf{p}^+(\mathbf{p}^*) = \mathbf{p}^*$, and so (32) implies,

$$c' \left(d_t + \sum_{n \in \mathcal{N}} u_{nt}^*(\mathbf{p}^*) \right) = p_t^*, \quad \text{for all } t \in \mathcal{T}. \quad (41)$$

The price converges to the generation marginal cost over the charging horizon.

It will now be shown that $\mathbf{u}^*(\mathbf{p}^*)$ is the efficient (socially optimal) charging strategy that minimizes the central optimization problem (11). Let $\omega^* = \|\mathbf{u}^*(\mathbf{p}^*)\|_1$. If $0 < \omega^* < \Gamma_n$ then by Theorem 4.1, $A_n^*(\mathbf{p}^*) = h'_n(\omega^*)$. According to Lemma 4.1,

$$p_t^* + g'_{nt}(u_{nt}^*(\mathbf{p}^*)) - h'_n(\omega^*) \begin{cases} = 0, & \text{if } u_{nt}^*(\mathbf{p}^*) > 0 \\ \geq 0, & \text{otherwise} \end{cases}$$

so (13) is satisfied.

If $\omega^* = 0$ then by Theorem 4.1, $A_n^*(\mathbf{p}^*) \geq h'_n(\omega^*)$. Also, in this case, $u_{nt}^*(\mathbf{p}^*) = 0$ for all $t \in \mathcal{T}$. Therefore, from Lemma 4.1,

$$p_t^* + g'_{nt}(u_{nt}^*(\mathbf{p}^*)) \geq A_n^*(\mathbf{p}^*) \geq h'_n(\omega^*)$$

which again satisfies (13).

Suppose $\omega^* = \Gamma_n$, then by Theorem 4.1, $A_n^*(\mathbf{p}^*) \leq h'_n(\omega^*) = 0$. There must exist at least one instant $t \in \mathcal{T}_n$ where $u_{nt}^* > 0$. At such an instant, Lemma 4.1 implies,

$$\begin{aligned} p_t^* + g'_{nt}(u_{nt}^*(\mathbf{p}^*)) - A_n^*(\mathbf{p}^*) &= 0 \\ \Rightarrow p_t^* + g'_{nt}(u_{nt}^*(\mathbf{p}^*)) &\leq 0 \end{aligned}$$

and so $p_t^* < 0$ because $g'_{nt}(u_{nt}^*(\mathbf{p}^*)) > 0$ according to Assumption (A2). However this is not possible, as Assumption (A1) ensures that $p_t^* > 0$ for all $t \in \mathcal{T}$. Hence, $\omega^* < \Gamma_n$, which is consistent with the efficient solution.

Therefore the collection of optimal PEV charging strategies is efficient, $\mathbf{u}^* = \mathbf{u}^{**}$, with respect to the converged price $\mathbf{p}^* = \mathbf{p}^{**}$.

Given $\alpha \equiv |1 - \eta| + 2N\kappa v \eta < 1$, (39) implies,

$$\|\mathbf{p}^{(k)} - \mathbf{p}^{**}\|_1 \leq \alpha^k \|\mathbf{p}^{(0)} - \mathbf{p}^{**}\|_1.$$

With $p_t^{(0)}, p_t^{**} \in [0, q_{max}]$ for all $t \in \mathcal{T}$, this gives,

$$\|\mathbf{p}^{(k)} - \mathbf{p}^{**}\|_1 \leq \alpha^k T q_{max},$$

which implies that $\|\mathbf{p}^{(k)} - \mathbf{p}^{**}\|_1 \leq \varepsilon$ for k satisfying (35). ■

5. Numerical illustrations

5.1. Convergence

This section provides an illustration of Algorithm 1 using parameter values that match those of Section 3.2. For the generation cost function (14), the marginal cost is given by,

$$p(y_t) = c'(y_t) = 5.8 \times 10^{-7} y_t + 0.06.$$

The corresponding Lipschitz constant is $\kappa = 5.8 \times 10^{-7}$. From (15), the Lipschitz constant for $[g'_{nt}]^{-1}(\cdot)$ is $v = 1/0.006 = 166.7$. Given these values,

$$\alpha \equiv |1 - \eta| + 2N\kappa v \eta = |1 - \eta| + 0.967\eta,$$

which is less than 1 whenever $0 < \eta < 1.017$. Thus by Corollary 4.1, the system is guaranteed to converge to the efficient solution for all $\eta \in (0, 1.017)$. It is straightforward to show that α is a minimum when $\eta = 1$, giving $\alpha = 0.967 < 1$.

With $\alpha = 0.967$, $T = 24$ and $q_{max} = 0.3$, Algorithm 1 will converge to a price profile \mathbf{p}^* , such that $\|\mathbf{p}^* - \mathbf{p}^{**}\|_1 < \varepsilon = 0.0001$, in less than $K = 334$ iterations, according to (35). Fig. 8 shows the evolution of $\|\mathbf{p}^{(k)} - \mathbf{p}^{**}\|_1$, with $\eta = 1$, from an initial price profile $p_t^{(0)} = c'(d_t)$ for all $t \in \mathcal{T}$, i.e. zero charging load. It can be seen that convergence to the desired tolerance is achieved in about 10 iterations, which is much less than the theoretical upper bound of 334.

As η increases over the range $0 < \eta \leq 1$, the value of α decreases, with (39) suggesting faster convergence of Algorithm 1. Fig. 9 shows this to be the case. Further increasing η results in α

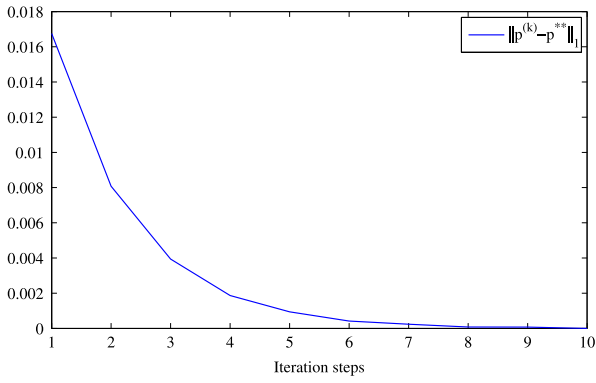


Fig. 8. Convergence of $\|p^{(k)} - p^{**}\|_1$ for Algorithm 1, with $\eta = 1$.

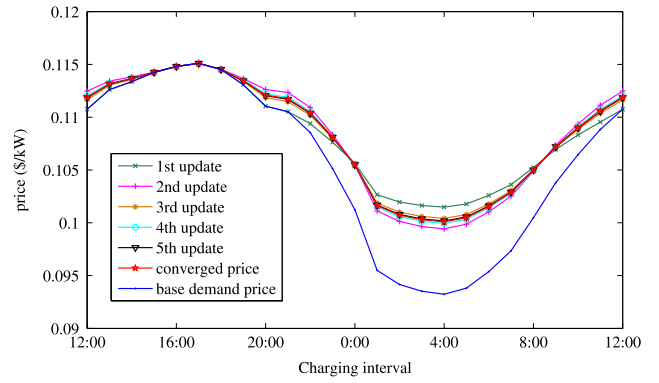


Fig. 11. Price profile updates achieved by Algorithm 1.

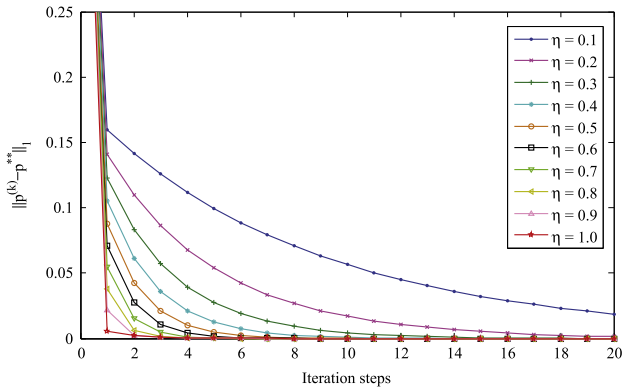


Fig. 9. Evolution of $\|p^{(k)} - p^{**}\|_1$ for values of η that satisfy the sufficient condition of Corollary 4.1.

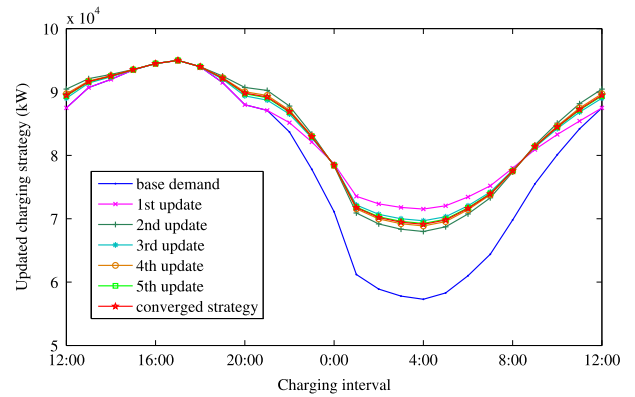


Fig. 12. Total demand at each iteration of Algorithm 1.

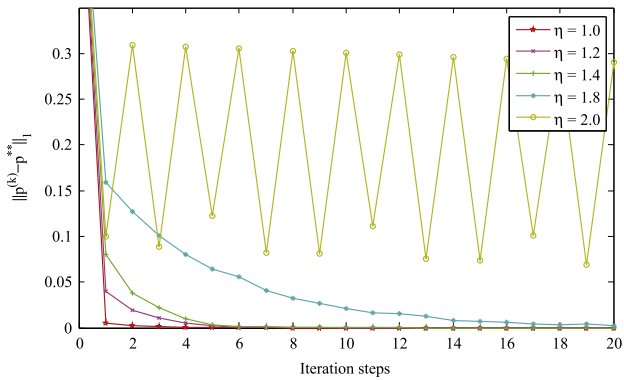


Fig. 10. Evolution of $\|p^{(k)} - p^{**}\|_1$, with the sufficient condition of Corollary 4.1 not satisfied for $\eta > 1.017$.

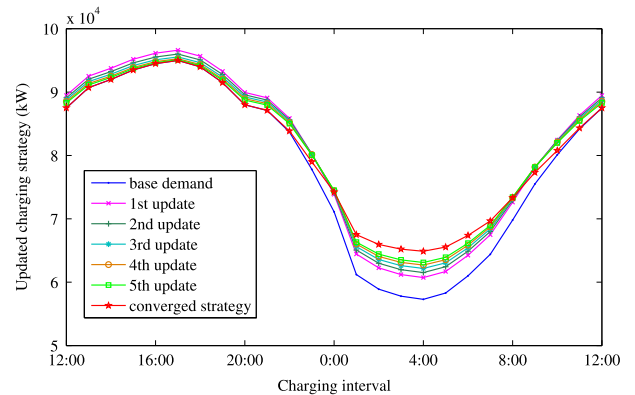


Fig. 13. Total demand at each iteration of Algorithm 1 for a heterogeneous PEV population.

increasing, with convergence only guaranteed while $\eta < 1.017$. Nevertheless, as shown in Fig. 10, the algorithm may still converge even when this sufficient condition is violated. It is also apparent, however, that larger values of η result in non-convergence, with oscillations occurring when $\eta = 2$.

The price profile updates achieved by Algorithm 1 are shown in Fig. 11, while Fig. 12 shows the corresponding total aggregate demand at each iteration. Note that the converged case in Fig. 12 corresponds exactly to the socially optimal strategy in Fig. 2.

5.2. Heterogeneity

To consider the effect of heterogeneity in the PEV population, suppose that the initial value of each PEV's SoC, soc_{i0} , satisfies a Gaussian distribution $N(\mu, \varrho)$ where $\mu = 50\%$ and $\varrho = 0.1$,

which is consistent with Luo, Hu, Song, Xu, and Lu (2013a,b). The total aggregate demand at each iteration of the update procedure is shown in Fig. 13. By adopting the proposed decentralized algorithm, the process converges to the efficient solution in a few iterations. Moreover, Fig. 14 illustrates the converged charging strategies for a sample of the heterogeneous PEVs.

5.3. Comparison with the algorithm of Gan et al. (2013)

The relative performance of Algorithm 1 will be illustrated through a comparison with the optimal decentralized charging algorithm of Gan et al. (2013) (referred to as GTL). The optimal charging strategy attained by the GTL algorithm is valley filling since the objective is to minimize the electricity cost over the charging horizon, and there are no battery degradation or demand

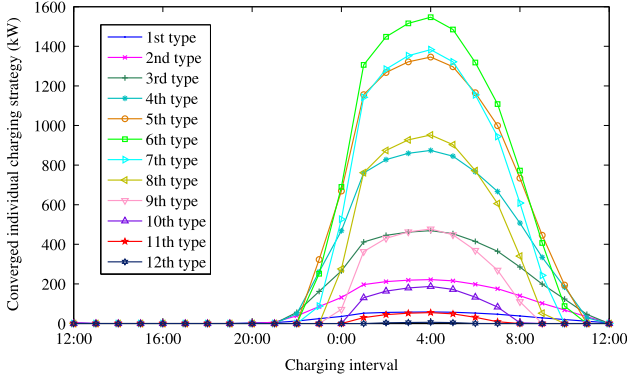


Fig. 14. Optimal charging strategies for individuals within a heterogeneous PEV population.

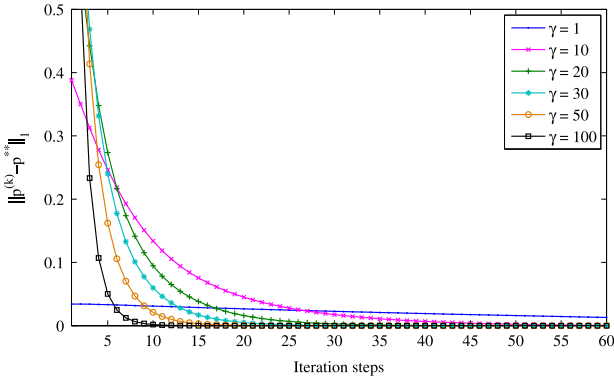


Fig. 15. Evolution of $\|\mathbf{p}^{(k)} - \mathbf{p}^{**}\|_1$ for the GTL algorithm for different values of γ .

costs involved. Also, GTL assumes that all PEVs are fully charged by the end of the charging period.

In order to provide a meaningful comparison with Algorithm 1, the GTL algorithm must be modified to take into account PEV utility (8). Accordingly, the optimal charging profile of each PEV is given by,

$$\mathbf{u}_n^{(k+1)}(\mathbf{u}_n^{(k)}, \mathbf{p}^{(k)}) \triangleq \underset{\mathbf{u}_n \in \mathcal{U}_n}{\operatorname{argmin}} \sum_{t \in \mathcal{T}} \left\{ p_t^{(k)} u_{nt} + g_{nt}(u_{nt}) \right\} + \frac{1}{2} \|\mathbf{u}_n - \mathbf{u}_n^{(k)}\|^2 - h_n \left(\sum_{t \in \mathcal{T}} u_{nt} \right). \quad (42)$$

The parameter values from Section 5.1 have again been used for generation cost and EV charging characteristics.

The GTL algorithm defines a parameter γ which governs the update process at each iteration,

$$p_t^{(k+1)} = \gamma c' \left(d_t + \sum_{n \in \mathcal{N}} u_{nt}^{(k+1)} \right).$$

Fig. 15 shows the evolution of $\|\mathbf{p}^{(k)} - \mathbf{p}^{**}\|_1$ for different values of γ . Compared with Fig. 9, Algorithm 1 provides faster convergence than the GTL algorithm.

The analysis in Gan et al. (2013) shows that convergence to the optimal strategy is guaranteed as the number of iterations approaches infinity. In contrast, Corollary 4.1 guarantees that Algorithm 1 will converge to an ε -optimal strategy in no more than $K(\varepsilon)$ iterations.

Next, the influence of the battery and demand charges on convergence performance will be demonstrated. This is achieved by setting $g_{nt}(\cdot)$ to zero in (42). Fig. 16 shows the evolution of $\|\mathbf{p}^{(k)} - \mathbf{p}^{**}\|_1$ for the GTL algorithm in this case. Comparison with Fig. 15 suggests that inclusion of the battery and demand costs tends to improve the convergence performance.

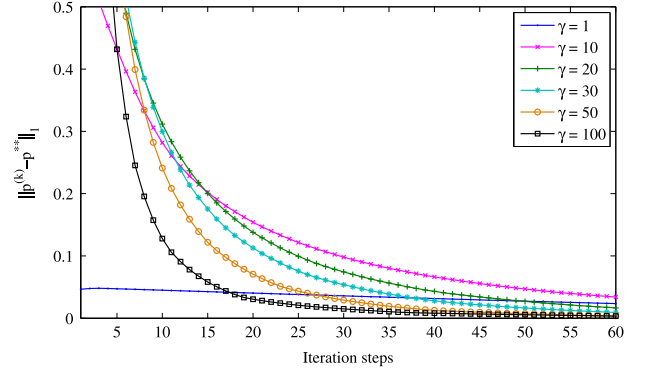


Fig. 16. Evolution of $\|\mathbf{p}^{(k)} - \mathbf{p}^{**}\|_1$ for the GTL algorithm without battery and demand costs.

6. Conclusions

A price-based strategy for coordinating the charging of a large population of PEVs has been formulated. The cost function underpinning the strategy establishes a tradeoff between the cost of energy and costs associated with battery degradation. It also introduces a charge that penalizes high demand, thereby mitigating occurrences of high coincident charging on local distribution grids. A decentralized scheme is proposed where all PEVs simultaneously update their optimal charging strategies with respect to a common price profile, and then the price profile is updated using these latest proposed charging strategies. The paper establishes sufficient conditions that ensure this iterative process converges to the unique efficient collection of charging strategies. At convergence, the price profile coincides with the generator marginal cost.

Appendix. Proof of Lemma 4.4

Recall that $\mathbf{u}_n^*(\mathbf{p}), \mathbf{u}_n^*(\mathbf{q}) \in \mathcal{U}_n$ represent the optimal response of the n th PEV with respect to price profiles \mathbf{p} and \mathbf{q} respectively,

$$\mathbf{u}_n^*(\mathbf{p}) \triangleq \min_{\mathbf{u}_n \in \mathcal{U}_n} J_n(\mathbf{u}_n; \mathbf{p}), \quad \mathbf{u}_n^*(\mathbf{q}) \triangleq \min_{\mathbf{u}_n \in \mathcal{U}_n} J_n(\mathbf{u}_n; \mathbf{q}).$$

Also, by Theorem 4.1,

$$\mathbf{u}_n^*(\mathbf{p}) = \mathbf{u}_n(\mathbf{p}, A_n^*(\mathbf{p})), \quad \mathbf{u}_n^*(\mathbf{q}) = \mathbf{u}_n(\mathbf{q}, A_n^*(\mathbf{q})).$$

For later analysis, it is useful to define another charging strategy for the n th PEV,

$$\vartheta_n(\mathbf{p}, \mathbf{q}) \equiv \mathbf{u}_n(\mathbf{q}, A_n^*(\mathbf{p})), \quad (43)$$

which is the charging strategy satisfying (18) with respect to \mathbf{q} and $A_n^*(\mathbf{p})$. Note that $\vartheta_n(\mathbf{p}, \mathbf{q})$ may not satisfy the admissibility constraint (1a). However, $\vartheta_n(\mathbf{p}, \mathbf{q})$ will only be used as a medium to establish a relationship between the pair of admissible charging strategies $\mathbf{u}_n^*(\mathbf{p})$ and $\mathbf{u}_n^*(\mathbf{q})$.

It is sufficient to show (34) if the following inequalities hold:

$$|u_{nt}^*(\mathbf{p}) - \vartheta_{nt}(\mathbf{p}, \mathbf{q})| \leq \nu |p_t - q_t|, \quad \forall t \in \mathcal{T} \quad (44)$$

$$\|\mathbf{u}_n^*(\mathbf{p}) - \mathbf{u}_n^*(\mathbf{q})\|_1 \leq 2\|\mathbf{u}_n^*(\mathbf{p}) - \vartheta_n(\mathbf{p}, \mathbf{q})\|_1. \quad (45)$$

These relationships will be verified in Appendices A.1 and A.2 respectively.

A.1. Verifying (44)

Firstly, consider the case where $u_{nt}^*(\mathbf{p}), \vartheta_{nt}(\mathbf{p}, \mathbf{q}) > 0$. It follows from (18), Theorem 4.1 and (43) that:

$$\begin{aligned} |u_{nt}^*(\mathbf{p}) - \vartheta_{nt}(\mathbf{p}, \mathbf{q})| &= |[g'_{nt}]^{-1}(A_n^*(\mathbf{p}) - p_t) - [g'_{nt}]^{-1}(A_n^*(\mathbf{p}) - q_t)| \\ &\leq \nu |p_t - q_t|, \end{aligned}$$

where the inequality holds by the specification of v given in (33). Following similar analysis, (44) holds for the other cases.

A.2. Verifying (45)

The proof of (45) will be established by considering three cases.

Case 1: $\|\vartheta_n(\mathbf{p}, \boldsymbol{\rho})\|_1 = \|\mathbf{u}_n^*(\mathbf{p})\|_1$

Let $\|\mathbf{u}_n^*(\mathbf{p})\|_1 = \bar{\omega}$ so that,

$$\|\vartheta_n(\mathbf{p}, \boldsymbol{\rho})\|_1 = \|\mathbf{u}_n(\boldsymbol{\rho}, A_n^*(\mathbf{p}))\|_1 = \bar{\omega}.$$

Then (26) implies $\mathcal{A}(\boldsymbol{\rho}, \bar{\omega}) = A_n^*(\mathbf{p})$. From (29),

$$\begin{aligned} f_n(\boldsymbol{\rho}, \bar{\omega}) &= \mathcal{A}(\boldsymbol{\rho}, \bar{\omega}) - h'_n(\bar{\omega}) \\ &= A_n^*(\mathbf{p}) - h'_n(\bar{\omega}) = f_n(\mathbf{p}, \bar{\omega}). \end{aligned}$$

It may be concluded from (30) that $A_n^*(\boldsymbol{\rho}) = A_n^*(\mathbf{p})$, and so $\vartheta_n(\mathbf{p}, \boldsymbol{\rho}) = \mathbf{u}_n(\boldsymbol{\rho}, A_n^*(\boldsymbol{\rho})) = \mathbf{u}_n^*(\boldsymbol{\rho})$. Consequently,

$$\begin{aligned} \|\mathbf{u}_n^*(\mathbf{p}) - \mathbf{u}_n^*(\boldsymbol{\rho})\|_1 &= \|\mathbf{u}_n^*(\mathbf{p}) - \vartheta_n(\mathbf{p}, \boldsymbol{\rho})\|_1 \\ &\leq 2\|\mathbf{u}_n^*(\mathbf{p}) - \vartheta_n(\mathbf{p}, \boldsymbol{\rho})\|_1. \end{aligned}$$

Case 2: $\|\vartheta_n(\mathbf{p}, \boldsymbol{\rho})\|_1 > \|\mathbf{u}_n^*(\mathbf{p})\|_1$.

The first step is to show that,

$$\|\vartheta_n(\mathbf{p}, \boldsymbol{\rho})\|_1 \geq \|\mathbf{u}_n^*(\boldsymbol{\rho})\|_1 \geq \|\mathbf{u}_n^*(\mathbf{p})\|_1. \quad (46)$$

This is achieved using proof by contradiction. Three subcases will be considered: (2A) $\|\mathbf{u}_n^*(\mathbf{p})\|_1 = \Gamma_n$, (2B) $0 < \|\mathbf{u}_n^*(\mathbf{p})\|_1 < \Gamma_n$, and (2C) $\|\mathbf{u}_n^*(\mathbf{p})\|_1 = 0$.

Case (2A): $\|\mathbf{u}_n^*(\mathbf{p})\|_1 = \Gamma_n$.

The charging strategy $\vartheta_n(\mathbf{p}, \boldsymbol{\rho})$ is not admissible since the total charging demand $\|\vartheta_n(\mathbf{p}, \boldsymbol{\rho})\|_1 > \Gamma_n$. Because $\mathbf{u}_n^*(\boldsymbol{\rho})$ must be admissible, $\|\mathbf{u}_n^*(\boldsymbol{\rho})\|_1$ cannot exceed $\|\mathbf{u}_n^*(\mathbf{p})\|_1 = \Gamma_n$. Therefore $\|\mathbf{u}_n^*(\boldsymbol{\rho})\|_1 < \|\vartheta_n(\mathbf{p}, \boldsymbol{\rho})\|_1$ which implies, by Lemma 4.2, that

$$A_n^*(\boldsymbol{\rho}) < A_n^*(\mathbf{p}). \quad (47)$$

To show that $\|\mathbf{u}_n^*(\boldsymbol{\rho})\|_1 = \|\mathbf{u}_n^*(\mathbf{p})\|_1$, assume $\|\mathbf{u}_n^*(\boldsymbol{\rho})\|_1 < \|\mathbf{u}_n^*(\mathbf{p})\|_1$. Then by (30) and the assumed condition $\|\mathbf{u}_n^*(\mathbf{p})\|_1 = \Gamma_n$, it follows that,

$$h'_n(\omega)|_{\omega=\|\mathbf{u}_n^*(\boldsymbol{\rho})\|_1} \leq A_n^*(\boldsymbol{\rho}) \quad (48a)$$

$$h'_n(\omega)|_{\omega=\|\mathbf{u}_n^*(\mathbf{p})\|_1} \geq A_n^*(\mathbf{p}). \quad (48b)$$

From (47) and (48),

$$h'_n(\omega)|_{\omega=\|\mathbf{u}_n^*(\boldsymbol{\rho})\|_1} < h'_n(\omega)|_{\omega=\|\mathbf{u}_n^*(\mathbf{p})\|_1},$$

which implies, by the concavity of h_n , that $\|\mathbf{u}_n^*(\boldsymbol{\rho})\|_1 > \|\mathbf{u}_n^*(\mathbf{p})\|_1$. However this contradicts the assumption $\|\mathbf{u}_n^*(\boldsymbol{\rho})\|_1 < \|\mathbf{u}_n^*(\mathbf{p})\|_1$. Hence,

$$\|\vartheta_n(\mathbf{p}, \boldsymbol{\rho})\|_1 > \|\mathbf{u}_n^*(\boldsymbol{\rho})\|_1 = \|\mathbf{u}_n^*(\mathbf{p})\|_1 = \Gamma_n.$$

Case (2B): $0 < \|\mathbf{u}_n^*(\mathbf{p})\|_1 < \Gamma_n$.

The desired result will be achieved by showing $\|\vartheta_n(\mathbf{p}, \boldsymbol{\rho})\|_1 \geq \|\mathbf{u}_n^*(\boldsymbol{\rho})\|_1$ in (2B.1), and $\|\mathbf{u}_n^*(\boldsymbol{\rho})\|_1 \geq \|\mathbf{u}_n^*(\mathbf{p})\|_1$ in (2B.2).

(2B.1) Suppose that,

$$\|\vartheta_n(\mathbf{p}, \boldsymbol{\rho})\|_1 < \|\mathbf{u}_n^*(\boldsymbol{\rho})\|_1. \quad (49)$$

Then $\|\mathbf{u}_n^*(\boldsymbol{\rho})\|_1 > 0$ because $\|\vartheta_n(\mathbf{p}, \boldsymbol{\rho})\|_1 > 0$. Also, Lemma 4.2 implies $A_n^*(\mathbf{p}) < A_n^*(\boldsymbol{\rho})$. Together with $0 < \|\mathbf{u}_n^*(\mathbf{p})\|_1 < \Gamma_n$ and (30), this gives,

$$\begin{aligned} h'_n(\omega)|_{\omega=\|\mathbf{u}_n^*(\mathbf{p})\|_1} &= A_n^*(\mathbf{p}) \\ &< A_n^*(\boldsymbol{\rho}) \leq h'_n(\omega)|_{\omega=\|\mathbf{u}_n^*(\boldsymbol{\rho})\|_1}. \end{aligned} \quad (50)$$

However, (49) and $\|\vartheta_n(\mathbf{p}, \boldsymbol{\rho})\|_1 > \|\mathbf{u}_n^*(\mathbf{p})\|_1$ together imply $\|\mathbf{u}_n^*(\boldsymbol{\rho})\|_1 > \|\mathbf{u}_n^*(\mathbf{p})\|_1$, and so,

$$h'_n(\omega)|_{\omega=\|\mathbf{u}_n^*(\boldsymbol{\rho})\|_1} \leq h'_n(\omega)|_{\omega=\|\mathbf{u}_n^*(\mathbf{p})\|_1} \quad (51)$$

by the concavity of h_n . This contradicts (50), indicating that the original assumption (49) was incorrect. Hence, $\|\vartheta_n(\mathbf{p}, \boldsymbol{\rho})\|_1 \geq \|\mathbf{u}_n^*(\boldsymbol{\rho})\|_1$.

(2B.2) Suppose that

$$\|\mathbf{u}_n^*(\boldsymbol{\rho})\|_1 < \|\mathbf{u}_n^*(\mathbf{p})\|_1. \quad (52)$$

Then $\|\mathbf{u}_n^*(\boldsymbol{\rho})\|_1 < \Gamma_n$, and $\|\mathbf{u}_n^*(\boldsymbol{\rho})\|_1 < \|\vartheta_n(\mathbf{p}, \boldsymbol{\rho})\|_1$ because $\|\vartheta_n(\mathbf{p}, \boldsymbol{\rho})\|_1 > \|\mathbf{u}_n^*(\mathbf{p})\|_1$. Hence, by Lemma 4.2, $A_n^*(\boldsymbol{\rho}) < A_n^*(\mathbf{p})$. Together with $0 < \|\mathbf{u}_n^*(\mathbf{p})\|_1 < \Gamma_n$ and (30), this gives,

$$\begin{aligned} h'_n(\omega)|_{\omega=\|\mathbf{u}_n^*(\boldsymbol{\rho})\|_1} &\leq A_n^*(\boldsymbol{\rho}) \\ &< A_n^*(\mathbf{p}) = h'_n(\omega)|_{\omega=\|\mathbf{u}_n^*(\mathbf{p})\|_1}. \end{aligned} \quad (53)$$

However, given the concavity of h_n , (52) implies,

$$h'_n(\omega)|_{\omega=\|\mathbf{u}_n^*(\boldsymbol{\rho})\|_1} > h'_n(\omega)|_{\omega=\|\mathbf{u}_n^*(\mathbf{p})\|_1}, \quad (54)$$

which contradicts (53). Hence, $\|\mathbf{u}_n^*(\boldsymbol{\rho})\|_1 \geq \|\mathbf{u}_n^*(\mathbf{p})\|_1$.

Case (2C): $\|\mathbf{u}_n^*(\mathbf{p})\|_1 = 0$.

Because $\mathbf{u}_n^*(\boldsymbol{\rho})$ is an admissible strategy, $\|\mathbf{u}_n^*(\boldsymbol{\rho})\|_1 \geq \|\mathbf{u}_n^*(\mathbf{p})\|_1 = 0$. Suppose that,

$$\|\vartheta_n(\mathbf{p}, \boldsymbol{\rho})\|_1 < \|\mathbf{u}_n^*(\boldsymbol{\rho})\|_1. \quad (55)$$

Then $\|\mathbf{u}_n^*(\boldsymbol{\rho})\|_1 > 0$. Also, Lemma 4.2 implies $A_n^*(\mathbf{p}) < A_n^*(\boldsymbol{\rho})$. Together with $\|\mathbf{u}_n^*(\mathbf{p})\|_1 = 0$ and (30), this gives,

$$\begin{aligned} h'_n(\omega)|_{\omega=\|\mathbf{u}_n^*(\mathbf{p})\|_1} &\leq A_n^*(\mathbf{p}) \\ &< A_n^*(\boldsymbol{\rho}) \leq h'_n(\omega)|_{\omega=\|\mathbf{u}_n^*(\boldsymbol{\rho})\|_1}. \end{aligned} \quad (56)$$

However, (55) together with $\|\vartheta_n(\mathbf{p}, \boldsymbol{\rho})\|_1 > \|\mathbf{u}_n^*(\mathbf{p})\|_1$ imply $\|\mathbf{u}_n^*(\boldsymbol{\rho})\|_1 > \|\mathbf{u}_n^*(\mathbf{p})\|_1$, giving,

$$h'_n(\omega)|_{\omega=\|\mathbf{u}_n^*(\mathbf{p})\|_1} \geq h'_n(\omega)|_{\omega=\|\mathbf{u}_n^*(\boldsymbol{\rho})\|_1}, \quad (57)$$

by the concavity of h_n . This contradicts (56), indicating that the assumption (55) was incorrect. Hence, $\|\vartheta_n(\mathbf{p}, \boldsymbol{\rho})\|_1 \geq \|\mathbf{u}_n^*(\boldsymbol{\rho})\|_1$.

Case 2 summary: It has been shown in Cases (2A)–(2C) that (46) holds. Because $\|\vartheta_n(\mathbf{p}, \boldsymbol{\rho})\|_1 \geq \|\mathbf{u}_n^*(\boldsymbol{\rho})\|_1$, Lemma 4.2 implies that $A_n^*(\boldsymbol{\rho}) \leq A_n^*(\mathbf{p})$, and therefore that,

$$0 \leq u_{nt}^*(\boldsymbol{\rho}) \leq \vartheta_{nt}(\mathbf{p}, \boldsymbol{\rho}), \quad (58)$$

for all $t \in \mathcal{T}$. Hence,

$$\begin{aligned} 0 &\leq \|\vartheta_n(\mathbf{p}, \boldsymbol{\rho}) - \mathbf{u}_n^*(\boldsymbol{\rho})\|_1 \\ &= \|\vartheta_n(\mathbf{p}, \boldsymbol{\rho})\|_1 - \|\mathbf{u}_n^*(\boldsymbol{\rho})\|_1 \quad \text{by (58)} \\ &\leq \|\vartheta_n(\mathbf{p}, \boldsymbol{\rho})\|_1 - \|\mathbf{u}_n^*(\mathbf{p})\|_1 \quad \text{by (46)} \\ &\leq \|\vartheta_n(\mathbf{p}, \boldsymbol{\rho}) - \mathbf{u}_n^*(\mathbf{p})\|_1 \end{aligned} \quad (59)$$

where the final inequality is due to the reverse triangle inequality. Therefore,

$$\begin{aligned} \|\mathbf{u}_n^*(\mathbf{p}) - \mathbf{u}_n^*(\boldsymbol{\rho})\|_1 &\leq \|\vartheta_n(\mathbf{p}, \boldsymbol{\rho}) - \mathbf{u}_n^*(\mathbf{p})\|_1 + \|\vartheta_n(\mathbf{p}, \boldsymbol{\rho}) - \mathbf{u}_n^*(\boldsymbol{\rho})\|_1 \\ &\leq \|\vartheta_n(\mathbf{p}, \boldsymbol{\rho}) - \mathbf{u}_n^*(\mathbf{p})\|_1 + \|\vartheta_n(\mathbf{p}, \boldsymbol{\rho}) - \mathbf{u}_n^*(\mathbf{p})\|_1 \\ &= 2\|\mathbf{u}_n^*(\mathbf{p}) - \vartheta_n(\mathbf{p}, \boldsymbol{\rho})\|_1, \end{aligned}$$

where the first inequality is due to the triangle inequality and the second is from (59).

Case 3: $\|\vartheta_n(\mathbf{p}, \mathbf{q})\|_1 < \|\mathbf{u}_n^*(\mathbf{p})\|_1$.

Following a similar approach to that adopted for Case 2, it can again be shown that (45) holds. \square

References

- Bashash, S., Moura, S., Forman, J., & Fathy, H. (2011). Plug-in hybrid electric vehicle charge pattern optimization for energy cost and battery longevity. *Journal of Power Sources*, 196, 541–549.
- Berinde, V. (2007). *Iterative approximation of fixed points*. Springer.
- Bompard, E., Ma, Y., Napoli, R., & Abrate, G. (2007). The demand elasticity impacts on the strategic bidding behavior of the electricity producers. *IEEE Transactions on Power Systems*, 22(1), 188–197.
- Boyd, S., & Vandenberghe, L. (2004). *Convex optimization*. Cambridge university press.
- Callaway, D., & Hiskens, I. (2011). Achieving controllability of electric loads. *Proceedings of the IEEE*, 99-1, 184–199.
- Cheng, K., Divakar, B., Wu, H., Ding, K., & Ho, H. F. (2011). Battery-management system (BMS) and SOC development for electrical vehicles. *IEEE Transactions on Vehicular Technology*, 60(1), 76–88.
- Clement-Nyns, K., Haesen, E., & Driesen, J. (2010). The impact of charging plug-in hybrid electric vehicles on a residential distribution grid. *IEEE Transactions on Power Systems*, 25(1), 371–380.
- Deliso, R. (2013). Understanding peak demand charges, EnerNOC EnergySMART, August.
- Denholm, P., & Short, W. (2006). *An evaluation of utility system impacts and benefits of optimally dispatched plug-in hybrid electric vehicles, technical report NREL/TP-620-40293*. National Renewable Energy Laboratory, October.
- Fan, Z. (2012). A distributed demand response algorithm and its application to PHEV charging in smart grids. *IEEE Transactions on Smart Grid*, 3(3), 1280–1290.
- Fernández, L., Román, T., Cossent, R., Domingo, C., & Frías, P. (2011). Assessment of the impact of plug-in electric vehicles on distribution networks. *IEEE Transactions on Power Systems*, 26(1), 206–213.
- Forman, J., Moura, S., Stein, J., & Fathy, H. (2012). Optimal experimental design for modeling battery degradation. In *Proceedings of dynamic systems and control conference* (pp. 309–318).
- Forman, J., Stein, J., & Fathy, H. (2013). Optimization of dynamic battery parameter characterization experiments via differential evolution. In *American control conference* (pp. 867–874). Washington, DC, USA.
- Galus, M., & Andersson, G. (2008). Demand management of grid connected plug-in hybrid electric vehicles (PHEV). In *IEEE energy 2030*, Atlanta, Georgia.
- Gan, L., Chen, N., Wierman, A., Topcu, U., & Low, S. (2013). Real-time deferrable load control: handling the uncertainties of renewable generation. In *Fourth international conference on future energy systems*. ACM.
- Gan, L., Topcu, U., & Low, S. (2012). Stochastic distributed protocol for electric vehicle charging with discrete charging rate. In *IEEE power & energy society general meeting* (pp. 1–8).
- Gan, L., Topcu, U., & Low, S. (2013). Optimal decentralized protocol for electric vehicle charging. *IEEE Transactions on Power Systems*, 28(2), 940–951.
- Gountis, V., & Bakirtzis, A. (2004). Bidding strategies for electricity producers in a competitive electricity marketplace. *IEEE Transactions on Power Systems*, 19(1), 356–365.
- Grammatico, S., Parise, F., Colombino, M., & Lygeros, J. (0000). Decentralized convergence to Nash equilibria in constrained deterministic mean field control. *IEEE Transactions on Automatic Control*. arXiv:1410.4421v2 (cond. accepted).
- Hadley, S., & Tsvetkova, A. (2008). *Potential impacts of plug-in hybrid electric vehicles on regional power generation, technical report ORNL/TM-2007/150*. Oak Ridge National Laboratory, January.
- Han, S., Han, S., & Sezaki, K. (2010). Development of an optimal vehicle-to-grid aggregator for frequency regulation. *IEEE Transactions on Smart Grid*, 1(1), 65–72.
- Hermans, R., Almassalkhi, M., & Hiskens, I. (2012). Incentive-based coordinated charging control of plug-in electric vehicles at the distribution-transformer level. In *Proceedings of the American control conference* (pp. 264–269). Montreal, Canada.
- Kelly, F., Maulloo, A., & Tan, D. (1998). Rate control for communication networks: Shadow prices, proportional fairness and stability. *Journal of the Operational Research Society*, 49(3), 237–252.
- Kelly, L., Rowe, A., & Wild, P. (2009). Analyzing the impacts of plug-in electric vehicles on distribution networks in British Columbia. In *Proceedings IEEE electrical power and energy conference*, Montreal, Canada.
- Kim, J., Seo, G.-S., Chun, C., Cho, B.-H., & Lee, S. (2012). OCV hysteresis effect-based SOC estimation in extended Kalman filter algorithm for an LiFePO₄/C cell. In *IEEE international electric vehicle conference* (pp. 1–5). Greenville, SC.
- Koyanagi, F., & Urieu, Y. (1997). Modeling power consumption by electric vehicles and its impact on power demand. *Electrical Engineering in Japan*, 120(4), 40–47.
- Lee, T., Bareket, Z., & Gordon, T. (2012). Stochastic modeling for studies of real-world PHEV usage: Driving schedule and daily temporal distributions. *IEEE Transactions on Vehicular Technology*, 61(4), 1493–1502.
- Lu, L., Han, X., Li, J., Hua, J., & Ouyang, M. (2013). A review on the key issues for lithium-ion battery management in electric vehicles. *Journal of Power Sources*, 226, 272–288.
- Luo, Z., Hu, Z., Song, Y., Xu, Z., & Lu, H. (2013a). Optimal coordination of plug-in electric vehicles in power grids with cost-benefit analysis—Part I: Enabling techniques. *IEEE Transactions on Power Systems*, 28(4), 3546–3555.
- Luo, Z., Hu, Z., Song, Y., Xu, Z., & Lu, H. (2013b). Optimal coordination of plug-in electric vehicles in power grids with cost-benefit analysis—Part II: A case study in China. *IEEE Transactions on Power Systems*, 28(4), 3556–3565.
- Ma, Z., Callaway, D., & Hiskens, I. (2013). Decentralized charging control of large populations of plug-in electric vehicles. *IEEE Transactions on Control Systems Technology*, 21(1), 67–78.
- Mohsenian-Rad, A.-H., & Leon-Garcia, A. (2010). Optimal residential load control with price prediction in real-time electricity pricing environments. *IEEE Transactions on Smart Grid*, 1(2), 120–133.
- Moura, S., Forman, J., Bashash, S., Stein, J., & Fathy, H. (2011). Optimal control of film growth in lithium-ion battery packs via relay switches. *IEEE Transactions on Industrial Electronics*, 58(8), 3555–3566.
- Prosini, P. (2005). Modeling the voltage profile for LiFePO₄. *Journal of The Electrochemical Society*, 152(10), A1925–A1929.
- Rahman, S., & Shrestha, G. (1993). An investigation into the impact of electric vehicle load on the electric utility distribution system. *IEEE Transactions on Power Delivery*, 8(2), 591–597.
- Samadi, P., Mohsenian-Rad, A., Schober, R., Wong, V., & Jatskevich, J. (2010). Optimal real-time pricing algorithm based on utility maximization for smart grid. In *Proceedings of 1st IEEE international conference on smart grid communications*, Gaithersburg.
- Singh, A., Izadian, A., & Anwar, S. (2013). Fault diagnosis of li-ion batteries using multiple-model adaptive estimation. In *39th annual conference of the IEEE industrial electronics society* (pp. 3524–3529). Vienna.
- Smart, D. (1974). *Fixed point theorems*. London, UK: Cambridge University Press.
- Sundstrom, O., & Binding, C. (2010). *Planning electric-drive vehicle charging under constrained grid conditions, technical report*. Switzerland: IBM–Zurich, August.
- Wang, J., Liu, P., Hicks-Garner, J., Sherman, E., Soukiazian, S., Verbrugge, M., Tataria, H., Musser, J., & Finamore, P. (2011). Cycle-life model for graphite-LiFePO₄ cells. *Journal of Power Sources*, 194(8), 3942–3948.
- Waraich, R., Galus, M., Dobler, C., Balmer, M., Andersson, G., & Axhausen, K. (2009). *Plug-in hybrid electric vehicles and smart grid: Investigations based on a micro-simulation, technical report 10.3929/ethz-a-005916811*. Switzerland: Institute for Transport Planning and Systems, ETH Zurich.
- Wen, F., & David, A. (2001). Strategic bidding for electricity supply in a day-ahead energy market. *Electric Power Systems Research*, 59, 197–206.
- Wu, C., Mohsenian-Rad, H., & Huang, J. (2012). Vehicle-to-aggregator interaction game. *IEEE Transactions on Smart Grid*, 3(1), 434–442.
- Yu, X. (2008). Impact assessment of PHEV charge profiles on generation expansion using energy modeling system. In *Proceedings IEEE power and energy society general meeting*, Pittsburgh, PA.



Zhongjing Ma received the B.Eng. degree from Nankai University, Tianjin, China, in 1997, the M.Eng. and Ph.D. degrees from McGill University, Montreal, QC, Canada, in 2005 and 2009, respectively, all in the area of systems and control. After a period as a postdoctoral research fellow with the Center of Sustainable Systems, the University of Michigan, Ann Arbor, he joined Beijing Institute of Technology, Beijing, China, in 2010, where he is currently an Associate Professor. He was an Engineer with the Institute of Automation Research, Shanxi, China. His research interests lie in the areas of optimal control, stochastic systems, and applications in the power and microgrid systems.



scenarios.

Suli Zou received her B.S. degree in Electrical Engineering and its Automation from Beijing Institute of Technology (BIT), in 2011. She is currently working towards a Ph.D. in School of Automation at BIT, majoring in Control Theory and Control Engineering. Her undergraduate work studied the optimal control of smart grids, as well as the economic operation of a microgrid system. Her main research interests lie in the distributed and dynamic control process, optimization and game-based analyses of power and smart grid systems, especially the efficient coordination of electric vehicles charging in different



Long Ran received the B.Eng. degree and the M.Eng. degree from Beijing Institute of Technology in 2011 and 2014 respectively. He was skilled in the power electronic systems, optimal control, and distributed control. He participated in some national research projects including the National Natural Science Funds. From 2014, he has been worked in the Electric Power Research Institute of State Grid in Chongqing, China, charged with the renewable energy research, power system and performance tests of power plants.



Xingyu Shi was born in Hunan Province, China, in 1989. He received his B.E. degree from Beijing Institute of Technology (BIT), Beijing, China, in 2011 and M.Sc. degree from BIT in 2014. He is currently working towards the Ph.D. degree at Hunan University, Changsha, China. His research interests lie in the optimization and stability control of smart grids.



Ian A. Hiskens is the Vennema Professor of Engineering in the Department of Electrical Engineering and Computer Science, University of Michigan, Ann Arbor. He has held prior appointments in the Queensland electricity supply industry, and various universities in Australia and the United States. His research interests lie at the intersection of power system analysis and systems theory, with recent activity focused largely on integration of renewable generation and controllable loads. Dr. Hiskens is actively involved in various IEEE societies, and is VP-Finance of the IEEE Systems Council. He is a Fellow of IEEE, a Fellow of Engineers Australia and a Chartered Professional Engineer in Australia.